

## Final author response

Sections 1 and 2 contain the final author response to the reviews from referee #1 and referee #2, respectively. In each section, each set of referee comment (RC) and corresponding author comment (AC) is identified by a number. Concerning the changes made to the original manuscript by the author (described within the author comments) in response to the referee comments, we refer the reader to the marked-up revised manuscript, which can be found at the end of this document, as well as the non-marked-up revised manuscript and supplementary information. Note that, for each change, we indicate the corresponding page and line numbers. However, note that line numbers are erroneous in the marked-up revised manuscript; this means that line numbers should only be considered in relation to the non-marked-up revised manuscript. Page numbers, on the other hand, are consistent between the marked-up and non-marked-up versions.

### 1. Final response to comments from Referee #1

#### 1.1

**RC:** The knowledge gap or research questions addressed by this manuscript are not clear.

[...]

First, the question is what is the real aim of the manuscript? I think that the authors should state more clearly the research question or hypothesis driving this study, than just focusing it as a new version or integration of WaterGAP. Which is the real aim of the study: 1) to quantify (or rather update or give other versions of) glacier and non-glacier contributions to sea level, with more emphasis on glacier or non-glacier?, 2) to validate TWSA from WaterGap with GRACE, to update WaterGap with the glacier module integration? It is not clear at all. I recommend a main focus, with appropriate redistributed weight across the manuscript.

[...]

The introduction should be restructured to really focus on the research question addressed, the identification of knowledge gaps and objectives specifically the knowledge gaps. Glaciers, water use, sea, ocean mass change. I know that combining all of these concepts together and reducing the state of the art to an introduction or discussion is not easy, but I think it is worth the effort. There are many efforts attempting to do similar objectives, with completely different methods, that should be mentioned (for glacier melt contributions, impoundment and withdrawals of water, etc). If GRACE is not the main objective, I suggest reducing considerably the emphasis on it in the introduction. Also, missing important references [...].

**AC:** The aim of the study was stated in L. 104–105 of the original manuscript:

*“Our assessment aimed at quantifying this contribution during the period 1948–2016, as well as identifying its main drivers and components.”*

However, we agree on the fact that the knowledge gaps, aims and research questions of the study need to be expressed in a more structured way and formulated more clearly. Therefore, we have conscientiously re-formulated the introduction, making sure that all of these elements are clearly addressed and that the connection between them is apparent (L. 30–107 / pg. 1–4). The emphasis on the comparison to GRACE has been reduced, since this is not the main focus of the study. The research questions have been clearly formulated in the form of a list (L. 92–100 / pg. 3–4). Note that the order of the research questions intends to convey that the long-term assessment of TWSA and individual components (research questions 1, 2, 3 and 4) is the main focus of the manuscript, whereas the validation of the applied modelling approach (research question 5) is a secondary focus that is indispensable, as only based on this validation can the reader judge the reliability of our assessment. The fact that the main focus is disaggregated into four research questions shows that this main focus is broad and points towards an exhaustive assessment of TWSA and individual components.

## 1.2

**RC:** I also think that the manuscript is too long, giving too much information on all models and related details, and limited in the discussion and comparison with other studies.

**AC:** We generally agree on the fact that the manuscript is too long. Therefore, we have shortened the introduction (L. 30–107 / pg. 1–4), the content related to models, data sets and methods (L. 108–290 / pg. 4–10) and the content of section 6.3 (Section 3.2.4 in revised manuscript / L. 449–479 / pg. 18–20). Table 1 has been rendered more compact through the usage of placeholders (pg. 9) and Table 5 (Table 4 in revised manuscript / pg. 18) has been shortened by moving part of the results to the supplementary information (Table S3 in the supplementary information / pg. 4). On the other hand, we disagree with the suggestion that our manuscript is limited in the discussion and comparison with other studies for the reasons stated in AC 1.3.

## 1.3

**RC:** Also, the authors need to put their results in the context of the urgency to understand TWSA and OMC that precisely requires these results.

[...]

And again, the discussion, a comparison with other works is necessary, and to put the results of the study in context. Some of the references I here mention could help, as many others. Discussion is completely missing. For instance, can these estimates be compared in some way with others? Anomalies related to water storage and/or consumption by irrigation and reservoir impoundment (Chao et al., 2008; Hoekstra and Mekonnen, 2012; Jaramillo and Destouni, 2015; Stefanie Rost et al., 2008), glacier contributions to oceans (Braithwaite and Raper, 2002; Giesen and Oerlemans, 2013; Huss and Hock, 2015; Jacob et al., 2012; Meier, 1984; Radić and Hock, 2014).

**AC:** We have rather extensively discussed our results in the light of other works. For instance, in section 6.1.1 (Section 4.11 in revised manuscript), we have compared our linear trends of TWSA, LGWSA, LWSA,  $LWSA_{\text{hum}}$  and  $LWSA_{\text{clim}}$  to estimates from multiple recently published studies (see Table 5 in revised manuscript). Furthermore, section 6.2 (Section 4.2 in revised manuscript) also contains numerous references to other studies.

In section 6.2.2 (Section 4.2.2 in revised manuscript), global glacier contributions to oceans are discussed (1) by referring to studies (Marzeion et al., 2015; Slangen et al., 2017) in which the results of the glacier model used in our study have already been compared to other models, including the ones from Radić et al. (2014) and Huss and Hock (2015), (2) by comparing our estimate to the one from Zemp et al. (2019), which provides the state-of-the-art observational baseline of global glacier contributions to oceans, and (3) by referring to the results of Hirabayashi et al. (2010), who evaluated the mean seasonality computed by their model in a comparable way to ours.

In section 6.2.3 (Section 4.2.3 in revised manuscript), we have compared our estimate of the contribution of global reservoir impoundment to oceans to the most comprehensive assessment done up to now (Wada et al., 2017), which is based on and updates the results of Chao et al. (2008). As to groundwater storage anomalies related to irrigation groundwater abstraction, we have discussed this in relation to other studies in a qualitative way only; we recognize that some quantitative comparison to other estimates is missing here. Thus, we have introduced a brief comparison between our estimate of groundwater depletion under 70% deficit irrigation over 2003–2016 to the estimate of van Dijk et al. (2014) over a similar period (L. 625–627 / pg. 25–26).

Some of the references that you mention can be of interest for qualitative discussion. Rost et al. (2008) quantified the impact of anthropogenic land cover change on the global terrestrial water balance by applying a dynamic global vegetation and water balance model (LPJmL). Their conclusions are of interest for the discussion about the implications of lacking this influence in our assessment due to the fact that WaterGAP does not include land cover change. Thus, we have introduced a reference to their study (L. 684–686 / pg. 27).

However, many other references are not very relevant or suitable for comparison in our opinion. For instance, the estimates reported by Jaramillo and Destouni (2015) are relative to 100 large basins which represent 35% of the global land area excluding Antarctica, and thus could not be compared to

our global-scale estimates. Moreover, given the fact that the manuscript is already very long, we prefer not to include too many further references.

As to the need of putting our results more in the context of urgency, this has been resolved by reformulating the knowledge gaps in the introduction.

#### 1.4

**RC:** I find also some issues with structure, that again, break the main thread and hide the really important results.

[...]

I have a feeling that Section 6.2 does not belong there, and it is also containing much information that it is not important and dilutes the main message of the manuscript, from my perspective. But again, I may be wrong, depending on the main aim of the article. Can much of it be moved to Supplementary information. Instead, a good discussion of the results and comparison with other studies could fill that gap.

**AC:** We consider that the content of section 6.3 (we assume that the referee comment refers to section 6.3 and not 6.2) should be left as part of the manuscript, rather than moved to the supplementary information. As mentioned in AC 1.1, our assessment of TWSA and individual components is intended to be exhaustive. Even if we did not disaggregate  $LWSA_{clim}$  into individual contributions (as opposed to  $LWSA_{hum}$ , which was disaggregated into  $LWSA_{res}$  and  $LWSA_{abs}$ ) due to technical limitations of the model and general complexity, we still intended to investigate the main drivers behind this component. This is now reflected by research question 4 (see AC 1.1). This being said, we agree that the placement of this section in terms of structure is not ideal, and thus have moved it from the discussion to the results (Section 3.2.4 in revised manuscript / L. 449–479 / pg. 18–20). Also, we have made the content of this section more concise. In general, the structure of the results (Section 3 in revised manuscript / L. 295–496 / pg. 11–21) and discussion (Section 4 in revised manuscript / L. 497–686 / pg. 21–27) sections has been reworked.

#### 1.5

**RC:** The methods section is very hard to read, or in other words, very hard to focus while reading it. I assume it starts in L. 120 and finishes in L. 330? This should be explicit.

[...]

The information on models and data sets is important and should be generally included in a methods section, but in this case, due to the massive amount of information due to the complexity of the study, I suggest just leaving the most important methods and sending the details to supplementary information. Also, because now the red thread is completely lost by the end of the methods, and since the objectives are not very clear in the introduction.

**AC:** We agree that the information on models and data sets should be part of the methods section. Therefore, we have merged sections 2 and 3, “Models and data” and “Methods”, respectively, into one section entitled “Models, data and methods” (Section 2 in revised manuscript / L. 108–290 / pg. 4–10). Concerning the amount of information on models, data sets and methods, we are of the opinion that most of it should remain in the main text, because it is necessary to understand the results. We are also encouraged to do so based on the feedback of referee #2, who states that, although the manuscript is very lengthy, the methods are well elaborated, and the technical details help readers understand and potentially replicate our work. Nevertheless, we have reduced the content as far as possible and have moved section 3.2 (“Pre-processing of gridded GGM output data”) to the supplementary information (Section S1.1 in supplementary information / pg. 1).

#### 1.6

**RC:** There are so many acronyms, too many, I would just use the most important ones. For example what is the purpose of OMC, it is not a variable.

**AC:** We agree that the vast number of acronyms makes it difficult for the reader to stay focused. Therefore, we have eliminated the use of the following acronyms, as they are not considered essential:

SLR (sea-level rise), OMC (ocean mass change), SWB (surface water bodies), SMB (surface mass balance) and GWD (groundwater depletion). Moreover, in Table 5 (Table 4 in revised manuscript / pg. 18), we have included both the long name and the corresponding acronym of each variable.

### 1.7

**RC:** The results...where do they start by the way, in Model evaluation? Also, are they focused on the comparison with GRACE? That is why I ask if that is the main aim of the article.

**AC:** In order to avoid confusions as to where the results begin, we have modified the structure by merging sections 4 and 5, “Model evaluation” and “Global water transfer from continents to oceans over the period 1948–2016”, respectively, into one common section entitled “Results” (Section 3 in revised manuscript / L. 295–496 / pg. 11–21).

### 1.8

**RC:** For figure 4 and 5, can I recommend an additional simple barplot figure showing the TWSA with and without the accounting of glacier melt, with uncertainty ranges?

**AC:** We are not sure what you meant here. Would the values (bars) represented in the barplot still represent the TWSA time series (i.e. one bar per month/year), or would they represent the linear trends of contribution of TWSA to ocean mass change over the period considered by the respective figure? In any case, for both Figure 4 and 5, we do not see how adding an additional barplot would help the understanding of the reader.

However, in the case of Figure 5, including a barplot alongside each graph with the corresponding linear trends over 1948–2016 would be beneficial. First of all, the barplot related to the upper graph (TWSA) would replace Table 4 in the manuscript and, in this way, contribute to save some space. Secondly, the barplot related to the bottom graph (TWSA components) would allow us to include these additional results. Thus, we have modified the figure accordingly (Figure 5 in revised manuscript / pg. 16).

### 1.9

**RC:** Another suggestion, a brief explanation somewhere how the term "anomaly" on land and change of mass in the ocean are related.

**AC:** We have introduced a sentence in the introduction to clarify the meaning of the term “anomaly” (L. 50–51 / pg. 2). Furthermore, we consider that the link between mass anomaly on land and change of mass in the ocean has already been made clear by, for example, having the following sentence in the caption of Table 3 (pg. 15):

*“Negative trends (mass loss) over the continents, expressed in millimetres of land water height (mm LWH, relative to the global continental area without the ice sheets 132.3.106 km<sup>2</sup>), translate to positive trends (mass gain) over the oceans, expressed in millimetres of sea level equivalent (mm SLE, relative to the global ocean area 361.0.106 km<sup>2</sup>).”*

### 1.10

**RC:** The conclusions should also pinpoint the main objectives of the introduction, and focus in what is really important.

**AC:** We have performed several modifications to the text (L. 688–716 / pg. 27–28). The main objectives, results and implications are clearly stated.

### 1.11

**RC:** The y-axis of Fig. 4 and 5 mean different things but have the same level or no level at all. The level is missing, only units, and complicates the understanding of the results.

**AC:** At the end of the caption of Fig. 4, it is explained that “Anomalies are relative to the mean over the period January 2006 to December 2015 and given in millimetres of land water height (mm LWH).” The same sentence is found in the caption of Fig. 5, on that the anomaly is relative to the annual value of 1948. We are not completely sure what you meant by “the same level or no level at all”, however we would say that the level (i.e. what a value of zero means) is well described by these sentences and the reference levels are different. We think it is better to not have the same reference level in both figures as the reference level in Fig. 4 is due to GRACE data availability only, while Fig. 5 is to show changes since the beginning of the study period.

#### 1.12

**RC:** L. 466 The word “contribution” is not appropriate here, I would delete it. In general, the use of the word “contribution” is very subjective, can you be more direct in its real meaning. What is a “contribution to ocean mass change” really, increase or decrease in ocean mass? Why is it an addition to the continents?

**AC:** We agree on the fact that the use of the term “contribution” throughout the manuscript can lead to some misunderstandings. This is because, in the original manuscript, we have used this term in relation to ocean mass change (“contribution to ocean mass change”) and to continental water storage change (“contribution to TWSA”). The expression “contribution to TWSA” was used when referring to mass changes of individual components of TWSA; in e.g. section 5.3 (Section 3.2.5 in revised manuscript), the water storage compartments that gain mass (e.g. reservoir) represent positive contributions to TWSA, whereas the ones that lose mass (e.g. glacier) represent negative contributions to TWSA. A positive (negative) contribution to TWSA is nothing more than a water mass gain (loss) in the continents, which translates into a negative (positive) contribution to ocean mass change.

To avoid confusions, in the revised manuscript we have only used the term “contribution” in relation to ocean mass change. Regarding TWSA, we simply refer to water mass gains or losses. The sentence mentioned in the RC has been modified accordingly (L. 423–424 / pg. 17).

#### 1.13

**RC:** On the other hand, Table 5 is too complicated due to the amount of numbers and acronyms and the lack of explanations, maybe a Figure could be more illustrative? Many of the components have not been introduced before. Same for Figure 7.

**AC:** In order to reduce the complexity of Table 5 (Table 4 in revised manuscript / pg. 18), we have shortened it by moving part of the results to the supplementary information (Table S3 in supplementary information / pg. 4) and included both the long name and the corresponding acronym of each variable.

On the other hand, we disagree with the suggestion that many of the components in Table 5 (Table 4 in revised manuscript) and Figure 7 (Figure 9 in revised manuscript) had not been introduced before. The components corresponding to the individual water storage compartments had already been introduced in section 2.1.2 (Section 2.2.1 in revised manuscript).

#### 1.14

**RC:** With losses, do you mean just negative anomalies?

**AC:** That is correct. Negative water storage anomalies in a given compartment indicate water mass losses in this compartment.

#### 1.15

**RC:** L. 22–25 What do these results have to do with the main aim of the article?

**AC:** The main aim of the article is to give an exhaustive long-term (1948–2016) assessment of TWSA and individual components. The results that you pointed out give the contribution of the  $LWSA_{res}$  and  $LWSA_{abs}$  components to ocean mass change over the considered period, while relating the large mass

decrease in the groundwater storage compartment to  $LWSA_{abs}$ . In addition, the  $LWSA_{clim}$  component is related to some of its main drivers. In the revised manuscript, these results answer research questions 2, 3 and 4 (see AC 1.1).

#### 1.16

**RC:** L. 31 – Missing reference (Chao, 2008)

**AC:** We have included the proposed reference in relation to the mentioned sentence (L. 33 / pg. 2).

#### 1.17

**RC:** L. 34–35 I don't see the purpose of this sentence.

**AC:** The purpose of this sentence is to introduce the mass component of sea-level change, i.e. ocean mass change. For the revised manuscript, the sentence has been slightly modified (L. 34–36 / pg. 2).

#### 1.18

**RC:** L138–140 So why are you using them then?

**AC:** The WFDEI climate forcing is not optimal for trend analysis due to varying station density in space and time related to the bias correction of monthly precipitation sums based on observation-based products (GPCC or CRU data). Despite this non-negligible caveat, WFDEI is still considered the state-of-the-art when it comes to large-scale hydrological impact studies. For instance, it has been used to force multiple impact models such as global hydrological models in the framework of the Inter-Sectoral Impact Model Intercomparison Project (<https://www.isimip.org>).

Adjusting reanalysis as e.g. ERA-Interim (WFDEI is based on this reanalysis data set) by observation-based products such as monthly GPCC or CRU precipitation allows for the consideration of additional data to scale the monthly sums while keeping the temporal daily variability of the reanalysis (Weedon et al., 2011; Weedon et al., 2014). Together with the snow undercatch corrections that are included in some of the state-of-the-art climate forcings (such as WFDEI), this renders hydrological impact studies more plausible. Müller Schmied et al. (2016) show in their Table 4 the effect of precipitation monthly bias correction, e.g. PGFv2.1 incorporating monthly CRU TS3.21, which results in a close match to initial CRU TS3.21 data, but also the effect of snow undercatch correction on the other climate forcings shown there. Kauffeldt et al. (2013) show in their Figure 8 that physically implausible runoff ratios would be obtained based solely on precipitation observations (CRU) in high-latitude or high-altitude areas without the implementation of a snow undercatch correction method. Hence, the inclusion of monthly observation-based precipitation data sets together with snow undercatch corrections improves the usability of such reanalyses.

In the case of GPCC, the data center provides a wide range of products. The typical product that is incorporated in reanalysis for hydrological impact studies (as e.g. WFDEI) is the so-called "Full Data Monthly" product, described as follows: "for the period 1891 to 2016 based on quality-controlled data from all stations in GPCC's data base available at the month of regard with a maximum number of more than 53,000 stations in 1986/1987. This product is optimized for best spatial coverage and use for water budget studies" (<https://www.dwd.de/EN/ourservices/gpcc/gpcc.html>). It is the most comprehensive data set (in both, space and time) they currently offer for advancing reanalysis at the given spatial resolution of 0.5°. A specifically dedicated product for trend analysis from GPCC is "HOMPRA Europe (V1)", described as follows: "a homogenized and quality-controlled data product suitable for trend analysis. The product is provided for the years 1951–2005 and is based on 5536 stations" (<https://www.dwd.de/EN/ourservices/gpcc/gpcc.html>). Even though this product is better suited for trend analysis, it is restricted to Europe and to the period 1951–2005, and thus not useful for most hydrological impact assessments.

To sum up, we justify our choice of climate forcing data sets by a) the lack of global-scale long-term precipitation measurements to generate time series that are specifically suited for trend analysis and b)

the raised value of reanalysis when additional precipitation observation data together with snow undercatch corrections are included. We agree that this is not well expressed in the manuscript and thus have added a sentence to clarify this (L. 124–127 / pg. 4).

## 2. Final response to comments from Referee #2

### 2.1

**RC:** My first concern is the selection of GRACE solutions. Obviously, GRACE solutions are important here as they were used as validation benchmarks. The authors applied the ensemble of four spherical harmonics (SH) solutions. I agree with the authors that the derived water storage trend can be sensitive to different GRACE solutions. Therefore, I wonder why the authors opted to only use SH solutions but not mascon solutions. Mascon solutions have merits in improved resolution and signal isolation. I am wondering what kind of influence the inclusion of mascon solutions will have on the model validation (I know some of the mascon solutions result in a smaller global trend, meaning the modeled LWSA trend even more overestimated). I would like to see more justifications, or at least a little discussion, about the selection of GRACE solutions.

**AC:** We agree that, in principle, mascons may be beneficial for many applications, especially in basin-scale analysis. However, this is not our use-case. Deploying mascons was initially discussed internally, but subsequently not considered for several reasons (without order):

- Being part of the ESA CCI Sea Level Budget Project (SLBC\_cci) let us aim for a complementary GRACE product to ocean mass change with preferably identical corrections and uncertainty assessment procedures, i.e. a degree-60 spherical-harmonics (SH) based approach that includes recent Glacial Isostatic Adjustment corrections after Caron et al. (2018), which is – to our knowledge – not available with mascons. In the meantime, there may be options without individual corrections included (e.g. CSR), but then the entire approach runs the risk of losing consistency.
- Mascons generally use geophysical a-priori constraints / regularization in space and time, which we find too interfering. The implementation of time-correlation as in JPL-RL06M introduces (small) changes to previous months after an update, which affects trend determination and comparability.
- We undertook an in-depth uncertainty assessment for the SH approach, which we understand much better than mascon uncertainties, where provided. Ours includes a combined time-dependent estimation of contributions from low-degree replacements (geo-center, flattening), GIA, leakage and noise, which lets us derive uncertainty ranges for individually picked temporal base-lines, as promoted in SLBC\_cci.
- One of the key elements in our GRACE continental solution is an oceanic leakage buffer: we implemented a dedicated procedure in order to integrate out-leaking signal over the oceanic area and correct for mean ocean change therein. For this, we need to employ a specific latitudinal-dynamic buffer mask (~300 km) that exactly nestles to the WGHM land-water mask. This is not easily accomplished with the mascons' dedicated masks, also not with JPL's CRI version. Even though mascons are (by design) not as affected by leakage as SH solutions, mascons would still require additional coastal processing due to fractional land-ocean separation. The mean-ocean-mass correction for such cells would require a product dedicated to ocean-mass and not ocean bottom pressure, as commonly provided with some mascon solutions. Adjusting for this effect is possible but, again, adds to inconsistencies in the overall approach.
- If gain factors were to be used, they could not be consistently applied in our global approach, as this also includes combined glacier- and hydrologically affected cells.

We could theoretically derive solutions solely based on mascons for comparison, yes. However, these would not fulfil our requirements in a consistent way. Therefore, we believe it would not be worth the

effort for this study. With regard to filtering and statistical noise-cancelling, we should also say that our approach is suitable for the global case, but may be significantly weaker in regional applications.

## 2.2

**RC:** Second, as the authors specified, the Caspian Sea is not included in WaterGAP, so the modelled LWSA excludes the impact of the level decline in the Caspian Sea (which can be substantial). The GRACE solutions, however, include the Caspian Sea in the land mask. I am unclear, at least given what the authors described, whether the GRACE TWSA used for model validation excludes the Caspian Sea or not. If not, the comparison wouldn't be apple-to-apple (GRACE TWSA with the Caspian Sea impact and modeled TWSA without), which leads to an even greater overestimation in the modelled water storage trend.

**AC:** Our GRACE continental mass change estimates do indeed include the Caspian Sea area. In our global approach, it would technically not be possible to treat it consistently as an ocean, primarily for the following reasons: (1) we extend the continental integration kernel onto the ocean area for leakage, but need to subtract the mean ocean change therefrom; which does not connect to the Caspian Sea for obvious reasons. (2) In recent versions of the ocean correction, we restore AOD1b (GAD) background models; which do not exist for the Caspian Sea, because it is not an ocean. And (3) if we wanted to apply the extended leakage-mask technique to the Caspian Sea, the latter would almost entirely be covered by the integration kernel and, hence, still contain the mass change signal. Which, in turn, would have to be corrected for unknown mean 'ocean' (Sea) mass change each month.

In order to address this issue, we have introduced a sentence that clarifies the fact that the GRACE-based solutions do include Caspian Sea mass changes (L. 676–677 / pg. 27) and performed a first-order evaluation of the possible trend difference between modelled TWSA and GRACE-based estimates by analysing the lake surface integration kernel (L. 677–679 / pg. 27). A brief description of how this first-order evaluation was performed, including two figures, has been incorporated in the supplementary information (Section S4 in supplementary information / pg. 4–6).

## 2.3

**RC:** Third, the modeled impact of reservoir water impoundment may be underestimated, particularly in the recent couple of decades. This is because WaterGAP incorporated the initial version of GRanD (version 1.1), rather than the updated version 1.3 that added another 458 large reservoirs mostly constructed after the year 2000. As a result, the modeled reservoir impact was underestimated after 2000. This underestimation was seen in Figure 6, where LWSA\_res flattens and declines during the recent decades. In addition, as the authors mentioned, GRanD only includes the largest reservoirs. Medium-sized and smaller reservoirs, such as partially documented in ICOLD, may add up to a substantial impoundment volume that was not taken into account in the model. These limitations (leading to underestimated LWSA\_res) ended up overestimating the declining trend in net human impacts (LWSA\_human). The authors may want to discuss more about these limitations about modeling reservoir impacts, and how they affect the conclusions.

**AC:** We thank you for this very pertinent comment. We recognize that the modelled impact of reservoir water impoundment is underestimated by the model, particularly during the last decades of the studied period, due to the fact that the additional reservoirs documented in GRanD v1.3, as compared to GRanD v1.1, are not accounted for by the model. There are ongoing efforts to incorporate these reservoirs in WaterGAP. However, this enhancement is still in progress and will only be available upon the release of the next model version. Therefore, as suggested by you, we have copiously discussed about this limitation and roughly estimated the possible trend difference that we would see if the additional reservoirs in GRanD v1.3 were taken into account in the model (L. 637–651 / pg. 26).



## 2.4

**RC:** Line 558: “closer to the estimate of Reager et al. (2016)”. I found this sentence far-fetching as the estimates of Reager et al. (-0.71 mm per year) and of the authors (-0.41 mm per year) have a difference of a factor of 2.

**AC:** We agree with this comment and have modified the mentioned sentence accordingly (L. 548–551 / pg. 23).

## 2.5

**RC:** Lines 660–661: This sentence can be misleading. 0.109 mm per year from 2002 to 2014 as reported in Wada et al. (2017), includes the contribution from both the surface water in the Caspian Sea and its influenced groundwater. 0.114 mm per year from 2002 to 2016 as reported in Wang et al. (2018), is the contribution of the entire Caspian Sea Basin, not the Caspian Sea alone. Based on Wang et al. (2018), the contribution of the Caspian Sea alone, i.e., the trend in its surface water volume, is 0.071 +/- 0.006 mm per year (or 25.52 +/- 2.12 Gt per year). For improved clarity, I recommend that the authors modify this sentence to be something like: “The contribution of this endorheic lake to SLR was estimated to 0.109 +/- 0.004 mm SLE per year (including variations in both surface water and the influenced groundwater) during the period 2002–2014 (Wada et al., 2017) and 0.071 +/- 0.006 mm SLE per year (including only surface water variation) during the period April 2002 to March 2016 (Wang et al., 2018).”

**AC:** We thank you for having pointed out this misinterpretation of ours. We have modified the sentence as proposed and included a trend reported by Milly et al. (2010) (0.06 mm yr<sup>-1</sup> SLE over 1992–2002) as well (L. 672–676 / pg. 27).

## References

- Caron, L., Ivins, E. R., Larour, E., Adhikari, S., Nilsson, J., and Blewitt, G.: GIA Model Statistics for GRACE Hydrology, Cryosphere, and Ocean Science, *Geophys. Res. Lett.*, 45, 2203–2212, doi:10.1002/2017GL076644, 2018.
- Chao, B. F., Wu, Y. H., and Li, Y. S.: Impact of artificial reservoir water impoundment on global sea level, *Science (New York, N.Y.)*, 320, 212–214, doi:10.1126/science.1154580, 2008.
- Hirabayashi, Y., Döll, P., and Kanae, S.: Global-scale modeling of glacier mass balances for water resources assessments: Glacier mass changes between 1948 and 2006, *Journal of Hydrology*, 390, 245–256, doi:10.1016/j.jhydrol.2010.07.001, 2010.
- Huss, M. and Hock, R.: A new model for global glacier change and sea-level rise, *Front. Earth Sci.*, 3, 382, doi:10.3389/feart.2015.00054, 2015.
- Jaramillo, F. and Destouni, G.: Local flow regulation and irrigation raise global human water consumption and footprint, *Science (New York, N.Y.)*, 350, 1248–1251, doi:10.1126/science.aad1010, 2015.
- Kauffeldt, A., Halldin, S., Rodhe, A., Xu, C.-Y., and Westerberg, I. K.: Disinformative data in large-scale hydrological modelling, *Hydrol. Earth Syst. Sci.*, 17, 2845–2857, doi:10.5194/hess-17-2845-2013, 2013.
- Marzeion, B., Leclercq, P. W., Cogley, J. G., and Jarosch, A. H.: Brief Communication: Global reconstructions of glacier mass change during the 20th century are consistent, *The Cryosphere*, 9, 2399–2404, doi:10.5194/tc-9-2399-2015, 2015.
- Milly, P. C. D. C., Cazenave, A., Famiglietti, J. S., Gornitz, V., Laval, K., Lettenmaier, D. P., Sahagian, D. L., Wahr, J. M., and Wilson, C. R.: Terrestrial Water-Storage Contributions to Sea-Level Rise and Variability, in: *Understanding Sea-level rise and variability*, Church, J. A. (Ed.), John Wiley & Sons, Chichester, 226–255, 2010.

- Müller Schmied, H., Adam, L., Eisner, S., Fink, G., Flörke, M., Kim, H., Oki, T., Portmann, F. T., Reinecke, R., Riedel, C., Song, Q., Zhang, J., and Döll, P.: Variations of global and continental water balance components as impacted by climate forcing uncertainty and human water use, *Hydrol. Earth Syst. Sci.*, 20, 2877–2898, doi:10.5194/hess-20-2877-2016, 2016.
- Radić, V., Bliss, A., Beedlow, A. C., Hock, R., Miles, E., and Cogley, J. G.: Regional and global projections of twenty-first century glacier mass changes in response to climate scenarios from global climate models, *Clim Dyn*, 42, 37–58, doi:10.1007/s00382-013-1719-7, 2014.
- Rost, S., Gerten, D., Bondeau, A., Lucht, W., Rohwer, J., and Schaphoff, S.: Agricultural green and blue water consumption and its influence on the global water system, *Water Resour. Res.*, 44, doi:10.1029/2007WR006331, 2008.
- Slangen, A. B. A., Adloff, F., Jevrejeva, S., Leclercq, P. W., Marzeion, B., Wada, Y., and Winkelmann, R.: A Review of Recent Updates of Sea-Level Projections at Global and Regional Scales, *Surv Geophys*, 38, 385–406, doi:10.1007/s10712-016-9374-2, 2017.
- van Dijk, A. I. J. M., Renzullo, L. J., Wada, Y., and Tregoning, P.: A global water cycle reanalysis (2003–2012) merging satellite gravimetry and altimetry observations with a hydrological multi-model ensemble, *Hydrol. Earth Syst. Sci.*, 18, 2955–2973, doi:10.5194/hess-18-2955-2014, 2014.
- Wada, Y., Reager, J. T., Chao, B. F., Wang, J., Lo, M.-H., Song, C., Li, Y., and Gardner, A. S.: Recent Changes in Land Water Storage and its Contribution to Sea Level Variations, *Surv Geophys*, 38, 131–152, doi:10.1007/s10712-016-9399-6, 2017.
- Weedon, G. P., Balsamo, G., Bellouin, N., Gomes, S., Best, M. J., and Viterbo, P.: The WFDEI meteorological forcing data set: WATCH Forcing Data methodology applied to ERA-Interim reanalysis data, *Water Resour. Res.*, 50, 7505–7514, doi:10.1002/2014WR015638, 2014.
- Weedon, G. P., Gomes, S., Viterbo, P., Shuttleworth, W. J., Blyth, E., Österle, H., Adam, J. C., Bellouin, N., Boucher, O., and Best, M.: Creation of the WATCH Forcing Data and Its Use to Assess Global and Regional Reference Crop Evaporation over Land during the Twentieth Century, *J. Hydrometeorol*, 12, 823–848, doi:10.1175/2011JHM1369.1, 2011.
- Zemp, M., Huss, M., Thibert, E., Eckert, N., McNabb, R., Huber, J., Barandun, M., Machguth, H., Nussbaumer, S. U., Gärtner-Roer, I., Thomson, L., Paul, F., Maussion, F., Kutuzov, S., and Cogley, J. G.: Global glacier mass changes and their contributions to sea-level rise from 1961 to 2016, *Nature*, 568, 382–386, doi:10.1038/s41586-019-1071-0, 2019.

# Assessing global water mass transfers from continents to oceans over the period 1948–2016

Denise Cáceres<sup>1</sup>, Ben Marzeion<sup>2</sup>, Jan Hendrik Malles<sup>2</sup>, Benjamin D. Gutknecht<sup>3</sup>, Hannes Müller Schmied<sup>1,4</sup>, Petra Döll<sup>1,4</sup>

5 <sup>1</sup>Institute of Physical Geography, Goethe University Frankfurt, Frankfurt am Main, Germany

<sup>2</sup>Institute of Geography and MARUM, University of Bremen, Germany

<sup>3</sup>Institut für Planetare Geodäsie, Technische Universität Dresden, Germany

<sup>4</sup>Senckenberg Leibniz Biodiversity and Climate Research Centre Frankfurt (SBiK-F), Frankfurt am Main, Germany

Correspondence to: Denise Cáceres (d.caceres@em.uni-frankfurt.de)

10 **Abstract.** Ocean mass and thus sea level is significantly affected by water storage on the continents. However, assessing the net contribution of continental water storage change to ocean mass change, remains a challenge. We present an integrated version of the WaterGAP global hydrological model that is able to consistently simulate total water storage anomalies (TWSA) over the global continental area (except Greenland and Antarctica), by integrating the output from the global glacier model of Marzeion et al. (2012) as an input to WaterGAP. Monthly time series of global mean TWSA obtained with an ensemble of four variants of the integrated model, corresponding to different precipitation input and irrigation water use assumptions, were validated against an ensemble of four TWSA solutions based on GRACE satellite gravimetry over 15 January 2003 to August 2016. With a mean Nash–Sutcliffe efficiency (NSE) of 0.87, simulated TWSA fit well to observations. By decomposing the original TWSA signal into its seasonal, linear trend and interannual components, we found that seasonal and interannual variability are almost exclusively caused by the glacier-free land water storage anomalies (LWSA). Seasonal amplitude and phase are very well reproduced (NSE = 0.88). The linear trend is overestimated by 30–50% (NSE = 0.65) and interannual variability is captured to a certain extent (NSE = 0.57) by the integrated model. During the period 1948–2016, we find that continents lost 34–41 mm of sea level equivalent (SLE) to the oceans, with global glacier mass loss accounting for 81% of the cumulated mass loss and LWSA, accounting for the remaining 19%. Over 1948–2016, the mass gain on land from impoundment of water in man-made reservoirs, equivalent to 8 mm SLE, was offset by the mass 25 loss from water abstractions, amounting to 15–21 mm SLE and reflecting a cumulated groundwater depletion of 13–19 mm SLE. Climate-driven LWSA are highly sensitive to precipitation input and correlate with El Niño Southern Oscillation multi-year modulations. Significant uncertainty remains in trends of modelled LWSA, which are highly sensitive to simulation of irrigation water use and man-made reservoirs.

**Deleted:** Continental water mass change affects ocean mass change (OMC)....

**Deleted:** A

**Deleted:** , however,

**Deleted:** continental

**Deleted:** consistently

**Deleted:** The overall fit to GRACE, measured by the

**Deleted:** coefficient, was found to be

**Deleted:** -

**Deleted:** in

**Deleted:** the s

**Deleted:** , t

**Deleted:** -

**Deleted:** glacier-free

**Deleted:** land water storage anomalies (

**Deleted:** )

## 1. Introduction

30 Global mean sea-level rise has been widely used as an indicator of the impact of climate change on the Earth system. In recent decades, it has mainly been caused by anthropogenic climate change (Slangen et al., 2016), but has also been affected by direct human interventions such as impoundment of water in man-made reservoirs and water abstractions on the

50 continents (Chao et al., 2008; Church et al., 2013; Oppenheimer et al., 2019). Since the beginning of the satellite altimetry era, several missions have produced continuous measurements of sea-level height to monitor its evolution. Primarily, sea-level change can be decomposed into a steric component (i.e. thermal expansion and salinity change) and a mass component (i.e. ocean mass change). Since the beginning of the 21<sup>st</sup> century, the Gravity Recovery and Climate Experiment (GRACE) mission has made the monitoring of spatially and temporally distributed ocean mass change possible. Moreover, according to the principle of water mass conservation in the Earth system, the latter can be estimated as the sum of temporal changes in mass of 1) Greenland and Antarctica ice sheets, 2) glaciers, 3) water stored on the continents (excluding glaciers) and 4) atmospheric water vapour. If the water mass in these four compartments decreases, ocean mass increases. A number of studies (Church et al., 2013; Chambers et al., 2017; Dieng et al., 2017; Cazenave, 2018) have shown that it is possible to reconstruct time series of global mean sea-level change by summing up changes in the individual components, within the uncertainties of the observational estimates. However, substantial uncertainty remains for individual components; this is the case of the net contribution of continental water storage change to ocean mass change, for which an accurate quantification continues to be a challenge (Cazenave, 2018). One way of assessing this contribution is through the usage of GRACE observations over the continents. However, GRACE observations cannot distinguish between mass changes of glaciers and of water stored elsewhere on the continents, such as soils, surface water bodies or groundwater, nor can reasons for mass changes be explored. In addition, GRACE records only start in 2002 and contain some temporal gaps.

60 In ocean mass budget studies, continental water storage change is usually decomposed into changes in mass of glaciers and of water stored in glacier-free land. To determine temporal mass changes, it is not necessary to compute time series of total mass but only time series of mass anomaly, i.e. mass variations as compared to a mean value over a specific time period. Hereafter, we refer to glacier mass as land glacier water storage anomaly (LGWSA), which does not include ice sheet peripheral glaciers, and to water mass on glacier-free land as land water storage anomaly (LWSA). LWSA is the sum of water stored in rivers, lakes, wetlands, man-made reservoirs, snow pack, canopy, soil and as groundwater, excluding glaciers (Church et al., 2013; Scanlon et al., 2018). It can also be disaggregated into a climate-driven ( $LWSA_{clim}$ ) and a human-driven component ( $LWSA_{hum}$ ). The sum of LGWSA and LWSA equals total continental water storage anomaly (TWSA).

65 The distinction between LGWSA and LWSA in ocean mass budget assessments stems partly from the fact that global glacier mass loss is known to be the main driver of water transfers from continents to oceans during the 20<sup>th</sup> century and the early 21<sup>st</sup> century (Zemp et al., 2019), and the rest of this century (Hirabayashi et al., 2013; Slangen et al., 2017; Hock et al., 2019). There are currently several global glacier models capable of simulating LGWSA at the global scale (Hirabayashi et al., 2013; Marzeion et al., 2012; Huss and Hock, 2015). LWSA can be derived from global hydrological and land surface models (GHMs). For instance, Munier et al. (2012) estimated LWSA for the period 1993–2009 over the global continental area by averaging the output of three GHMs. On the other hand, various other approaches have been employed to estimate LWSA. Dieng et al. (2015) used a global ocean mass budget approach over 2003–2013; they compared GRACE-based ocean mass change to the sum of mass components derived from independent products, except for LWSA, which was the

unknown quantity to be estimated. In other studies, this component was extracted from GRACE-derived TWSA (Reager et al., 2016; Rietbroek et al., 2016). Wada et al. (2017) assessed components of LWSA based on 1) modelling groundwater depletion with PCR-GLOBWB, 2) estimating impoundment behind dams by adding storage capacities of reservoirs (updated from Chao et al., 2008), 3) assuming the  $LWSA_{clim}$  estimate of Reager et al. (2016) and 4) very roughly estimating storage losses in endorheic lakes (Caspian Sea and Aral Sea), wetlands and due to deforestation based on literature. Because LWSA involves multiple water storage compartments and is not only driven by climate variability and change ( $LWSA_{clim}$ ) but also human activities ( $LWSA_{hum}$ ), its assessment remains highly uncertain.

To fill this key knowledge gap related to the TWSA and, more particularly, the LWSA component of ocean mass change, we did a long-term (1948–2016) assessment of TWSA over the global continental area (except Antarctica and Greenland). Our assessment provides not only the total contribution of continents to oceans but also quantifies the separate contributions of the individual components of TWSA. In a first instance, we disaggregated TWSA into the contributions of LGWSA,  $LWSA_{clim}$  and  $LWSA_{hum}$  (the sum of the latter two components is equal to LWSA). We further disaggregated  $LWSA_{hum}$  by quantifying separately the effect of water impoundment in reservoirs ( $LWSA_{res}$ ) and the effect of water abstraction ( $LWSA_{abs}$ ), and related  $LWSA_{clim}$  to global annual precipitation and to El Niño Southern Oscillation (ENSO). TWSA estimates were obtained by combining two state-of-the-art global models; the global glacier model GGM of Marzeion et al. (2012) and the GHM WaterGAP (Döll et al., 2003; Müller Schmied et al., 2014; Müller Schmied et al., 2016). In its standard version, WaterGAP simulates storage changes in all compartments except glaciers. Areas that in reality are covered by glaciers (hereafter glacierized areas) are treated as normal (i.e. non-glacierized) areas. To account for glacierized areas and the effect of glacier mass variability on water flow dynamics on the continents, we integrated  $0.5^\circ$  gridded annual time series of glacier area and monthly time series of LGWSA simulated by GGM as an input to WaterGAP. This resulted in a non-standard version of WaterGAP which includes the impact of glaciers on water storages and flows, hereafter referred to as integrated WaterGAP. The model was run with two different precipitation forcings and two different assumptions regarding irrigation water use, resulting in an ensemble of four solutions. We regarded the spread of these four time series around the ensemble mean as an informal indication of uncertainty. We validated the ensemble by comparing it to an ensemble of four GRACE spherical harmonics (SH) solutions. Through this comprehensive assessment, we aimed to address the following questions:

1. How did changes of total water storage on the continents of the Earth (except Greenland and Antarctica) contribute to ocean mass changes (and thus sea-level change) during the period 1948–2016? (Section 3.2.1)
2. Which continental storages underwent the most significant mass changes during this period? (Sections 3.2.2 and 3.2.5)
3. How have man-made reservoirs and human water abstractions affected water storage on the continents? (Section 3.2.3)
4. What were the main climatic drivers of glacier-free land water storage changes? (Section 3.2.4)

115 5. To what extent can we rely on our modelling approach to quantify global-scale water storage changes on the continents? (Sections 3.1 and 4.2)

Our assessment is innovative regarding 1) the modelling approach, which combines the strengths of two well-established global models, 2) the validation approach, which consisted in comparing TWSA over the global continental area from modelling and GRACE in terms of seasonality, linear trend and interannual variability, and 3) the disaggregation of TWSA into individual mass components and drivers.

In the following section, we describe the models, data sets and methods used in this study. In section 3, we present the results of our model validation and of our assessment of global TWSA over 1948–2016. The results are discussed in section 4. Finally, we present our conclusions in section 5.

## 2. Models, data and methods

### 2.1 Models

#### 2.1.1 Global hydrological model

We used the latest version of the GHM WaterGAP, WaterGAP2.2d. It simulates human water use as well as daily water flows and water storages (or anomalies) on a 0.5° by 0.5° grid (55 km by 55 km at equator and ~3000 km<sup>2</sup> grid cell) covering the global continental area except for Antarctica (see Fig. 1 in Döll et al., 2014). Streamflow is laterally routed through the stream network derived from the global drainage direction map DDM30 (Döll and Lehner, 2002) until it reaches the ocean or an inland sink. Calibration is performed against observations of mean annual streamflow at 1319 gauging stations (Müller Schmied et al., 2014). Daily climatological input data sets of precipitation, near-surface air temperature and long- and short-wave downwards surface radiation are required as input. We used a homogenized climate forcing (hereafter referred to as WFDEI) resulting from the combination of WATCH Forcing Data based on ERA-40 reanalysis (WFD, Weedon et al., 2011) for the period 1948–1978 and WFD methodology applied to ERA-Interim reanalysis (WFDEI, Weedon et al., 2014) for the period 1979–2016 (Müller Schmied et al., 2016). Monthly sums of precipitation are bias corrected by monthly precipitation data sets derived from raingage observations of either GPCC v5/v6 (Global Precipitation Climatology Centre, Schneider et al., 2015) or CRU TS3.10/TS3.21 (Climate Research Unit, Harris et al., 2014). Note that the GPCC and CRU products used to scale monthly precipitation sums within WFDEI use the available number of stations for each month. The variability in the number of observations over time makes the resulting precipitation data sets less suitable for trend analysis. However, as we are not aware of an available long-term global precipitation data set with high station density that could be used instead, note that the benefits of including those adjustments into reanalysis products due to e.g. the incorporation of snow undercatch corrections result in more plausible hydrological studies (Kauffeldt et al., 2013; Müller Schmied et al., 2016). We forced WaterGAP with both WFDEI with monthly precipitation sums based on GPCC (hereafter WFDEI-GPCC) and on CRU (hereafter WFDEI-CRU) to account for part of the uncertainty due to precipitation input data.

#### Moved (insertion) [13]

**Deleted:** Global mean sea-level rise (SLR) in recent decades is mainly caused by anthropogenic climate change (Slangen et al., 2016), but is also affected by direct human interventions such as impoundment of water in man-made reservoirs and water abstractions (Chao et al., 2008; Church et al., 2013; Oppenheimer et al., 2019) abstractions (Church et al., 2013; Oppenheimer et al., 2019). Since the beginning of the altimetry era, several satellite missions have produced continuous measurements of sea-level height to monitor its evolution. These records have given rise to multiple studies on global mean sea-level change and its different components (Gregory et al., 2013; Cazenave et al., 2014; Dieng et al., 2017). It is well-known that sea-level change can be decomposed into a steric component (i.e. thermal expansion and salinity change) and a mass component (i.e. change of ocean mass). The Gravity Recovery and Climate Experiment (GRACE) joint mission of the National Aeronautics and Space Administration (NASA) and the German Aerospace Center has enabled, for the first time in history, the monitoring of spatially and temporally distributed ocean mass change (OMC). The GRACE twin satellites have produced records of the Earth's gravity field anomalies extending from April 2002 to August 2016. Time series of OMC can be derived from the gravity field observations, upon applying several post-processing corrections to the raw data, e.g. regarding glacial isostatic adjustment and leakage from the continental mass signal. According to the principle of water mass conservation in the Earth system, OMC can be decomposed into temporal changes in mass of 1) Greenland and Antarctica ice sheets, 2) glaciers, 3) water stored on the continents and 4) atmospheric water vapour. If the water mass in these four compartments decreases, ocean mass increases. Hereafter, we refer to water mass changes of glaciers (different from ice sheet peripheral glaciers) as land glacier water storage anomaly (LGWSA) and the water mass changes on glacier-free land as land water storage anomaly (LWSA). LWSA is defined as all water stored in rivers, lakes, wetlands, man-made reservoirs, snow pack, canopy, soil and aquifers, excluding glaciers (Church et al., 2013; Scanlon et al., 2018). The sum of LGWSA and LWSA is equal to the total continental water storage anomaly (TWSA). The term anomaly is used to express that the absolute mass of water in glaciers and on glacier-free land is not known and also not relevant for determining the contribution of these mass changes to OMC. The sum of LGWSA and LWSA is equal to the total continental water storage anomaly (TWSA). It can be assumed that the majority of any mass decrease in TWSA leads to increased mass in the ocean in particular due to the small water storage capacity of the atmosphere (Dieng et al., 2015; Cazenave, 2018). TWSA and thus global water mass transfers from

**Moved up [13]:** The sum of LGWSA and LWSA is equal to the total continental water storage anomaly (TWSA). It can be assumed

**Deleted:** (Dieng et al., 2015; Cazenave, 2018). TWSA and thus global water mass transfers from continents to oceans can be derived either from estimates of its two components or from GRACE observations over the continents. LGWSA constitutes a major contribution to OMC. There are several global glacier models capable of simulating LGWSA at global scale (Hirabayashi et al., 2013; Marzeion et al., 2012; Huss and Hock, 2015). Using such a model, Marzeion et al. (2015) estimated a global glacier mass loss corresponding to  $63.2 \pm 7.9$  mm SLE between 1902 and 2005. Projections for the twenty-first century show that mass loss of glaciers will continue to be a significant contribution to OMC and thus SLR (Slangen et al., 2017; Hock et al., 2019). The contribution

**Deleted:** studies (Müller Schmied et al., 2016).

... [3]

260 WaterGAP simulates the impact of water impoundment in reservoirs and of human water use on water flows and storages.  
LWSA<sub>hum</sub> is calculated following Eq. (1):

$$LWSA_{hum} = LWSA_{res} + LWSA_{abs.} \quad (1)$$

265 where LWSA<sub>res</sub> is the anomaly due to impoundment of water in reservoirs and LWSA<sub>abs</sub> is the anomaly due to water  
abstraction. Reservoir data used by the model comes from a preliminary version of the Global Reservoir and Dam (GRanD)  
270 data base which includes 6862 reservoirs with a total storage capacity of 6197 km<sup>3</sup> (Lehner et al., 2011). The simulation of  
reservoir operation is based on a slightly modified version of the algorithm of Hanasaki et al. (2006), which distinguishes  
between irrigation and non-irrigation reservoirs (Döll et al., 2009). The model distinguishes between man-made reservoirs  
and regulated lakes (i.e. natural lakes whose outflows are regulated by a dam). Reservoirs (i.e. man-made reservoirs plus  
regulated lakes) are classified as “local”, meaning that they are fed only by runoff produced within the cell, or “global”,  
275 meaning that they are also fed by streamflow from the upstream cell. They are assumed to be global if their maximum  
storage capacity is at least 0.5 km<sup>3</sup> or their surface area is at least 100 km<sup>2</sup>. Since global reservoirs may spread over more  
than one grid cell, their water balance is computed in the outflow cell. Local lakes and local reservoirs within one cell are  
lumped into one local lake. Lumping multiple local reservoirs within one cell into one local reservoir inevitably erases the  
specific characteristics of each reservoir; the resulting lumped local reservoir is then not expected to be better simulated by  
280 the reservoir algorithm than by the lake one (Döll et al., 2009). In total, 1082 global man-made reservoirs and 85 global  
regulated lakes, which together represent a total storage capacity of 5764 km<sup>3</sup> (~16 mm SLE), are simulated by WaterGAP  
using the reservoir algorithm. The reservoir filling phase upon construction is simulated based on the first operational year  
and the storage capacity. The monthly release flow of irrigation reservoirs varies according to the downstream consumptive  
water use (i.e. part of water abstractions that evapotranspires during use). For non-irrigation reservoirs, it is assumed that the  
release flow remains unchanged throughout the year if the storage capacity to mean total annual outflow ratio is larger than  
0.5, while it otherwise depends, also in case of irrigation reservoirs, on daily inflows into the reservoir.

Concerning human water use, in a first instance, time series of water abstraction and consumptive water use are generated  
for five water use sectors (irrigation, livestock farming, domestic use, manufacturing industries and cooling of thermal power  
plants) by separate global water use models. The calculation of irrigation water use takes into account climate variability as  
285 well as yearly country estimates of irrigated area (Döll et al., 2012). The outputs of the water use models are then translated  
into net abstraction (i.e. total abstraction minus return flow) by the sub-model GWSWUSE, which distinguishes the source  
of abstracted water (surface water or groundwater). The net abstraction time series are then subtracted from the surface water  
and groundwater storage compartments of WaterGAP, respectively (Müller Schmied et al., 2014; Döll et al., 2014).

### 2.1.2 Global glacier model

290 We used the global glacier model GGM of Marzeion et al. (2012). The model computes mass changes of individual glaciers  
for the whole globe. It combines a glacier surface mass balance model, following an empirically based temperature-index

#### **Moved (insertion) [7]**

**Deleted:** WaterGAP represents the transport of water on continents as flows among a series of individual water storage compartments (see Figure 1 in Döll et al., 2014). It includes all continental water storage compartments except for glaciers. Thus, glacierized areas are treated as non-glacierized areas. LWSA, which integrates the changes in all the compartments, is calculated following Eq. (2):  
 $LWSA = SnWSA + CnWSA + SMWSA + GWSA + LaWSA + ReWSA + WeWSA + RiWSA$ , →→→ (2)  
where WSA is water storage anomaly in snow (Sn), canopy (Cn), soil moisture (SM), groundwater (G), lake (La), reservoir (Re), wetland (We) and river (Ri) storages.

**Deleted:** (see Figure 1 in Döll et al., 2014). It includes all continental water storage compartments except for glaciers. Thus, glacierized areas are treated as non-glacierized areas. LWSA, which integrates the changes in all the compartments, is calculated following Eq. (2):  
 $LWSA = SnWSA + CnWSA + SMWSA + GWSA + LaWSA + ReWSA + WeWSA + RiWSA$ , →→→ (2)  
where WSA is water storage anomaly in snow (Sn), canopy (Cn), soil moisture (SM), groundwater (G), lake (La), reservoir (Re), wetland (We) and river (Ri) storages.

**Deleted:** . It includes all continental water storage compartments except for glaciers. Thus, glacierized areas are treated as non-glacierized areas. LWSA, which integrates the changes in all the compartments, is calculated following Eq. (2):  
 $LWSA = SnWSA + CnWSA + SMWSA + GWSA + LaWSA + ReWSA + WeWSA + RiWSA$ , →→→ (2)  
where WSA is water storage anomaly in snow (Sn), canopy (Cn), soil moisture (SM), groundwater (G), lake (La), reservoir (Re), wetland (We) and river (Ri) storages.

325 approach, with a model that accounts for the response of glacier geometry (in the model defined by area, length and elevation range) to changes in glacier mass. The dynamic simulation of this response follows an area-volume-time scaling approach, based on the equation of Bahr et al. (1997), enabling the model to account for various feedbacks between glacier geometry and mass balance. The model is calibrated by fitting simulated glacier surface mass balance to observations from the collections of the World Glacier Monitoring Service (2016). The error in modelled annual glacier mass change is determined using a cross-validation routine applied to glaciers with observed mass balances.

330 GGM is forced by global time series of near-surface air temperature and precipitation fluxes. For this study, we used the mean of an ensemble of seven global gridded atmospheric data sets (New et al., 2002; Saha et al., 2014; Compo et al., 2011; Dee et al., 2011; Kobayashi et al., 2015; Poli et al., 2016; Gelaro et al., 2017), as choosing the ensemble mean over any of the individual data sets allows reducing the uncertainty due to input climate forcing data. As initial conditions, it also requires information on glacier area and minimum and maximum elevation, which are taken from the Randolph Glacier Inventory (RGI) version 6.0 (updated from Pfeffer et al., 2014). GGM includes both local (i.e. glacier-specific) and global parameters. Local parameters are calibrated and cross-validated following the procedure described in Marzeion et al. (2012). Global parameters are optimized following a multi-objective optimization routine, maximizing temporal correlation of model results and observations, and minimizing the model bias as well as the difference of the variance of modelled and observed mass balances.

## 2.2 Data

340 By combining WaterGAP, capable of simulating LWSA (Section 2.2.1), and GGM, capable of simulating LGWSA (Section 2.2.2), through a data integration approach (Section 2.3.1), we obtained global time series of TWSA and individual components at monthly scale over 1948–2016. We evaluated the LGWSA data set against annual and seasonal time series of glacier mass change from in situ observations (Section 2.2.3). The modelled global TWSA time series were evaluated using global GRACE-derived TWSA time series at monthly scale covering the period from January 2003 to August 2016, with some months with missing data in between (Section 2.2.4).

### 2.2.1 Modelled LWSA

345 WaterGAP simulates the transport of water on continents as flows among all continental water storage compartments except for glaciers (see Figure 1 in Döll et al., 2014). Glacierized areas are treated as non-glacierized areas. LWSA is calculated following Eq. (2):

$$LWSA = SnWSA + CnWSA + SMWSA + GWSA + LaWSA + ReWSA + WeWSA + RiWSA \quad (2)$$

350 where WSA is water storage anomaly in snow (Sn), canopy (Cn), soil moisture (SM), groundwater (G), lake (La), reservoir (Re), wetland (We) and river (Ri) storages.

#### Moved (insertion) [8]

**Deleted:** GGM computes glacier mass change at the scale of individual glaciers worldwide. In the framework of this study, the data were provided on a rectangular 0.5° by 0.5° grid (for consistency with WaterGAP spatial resolution) covering the entire globe (excluding the peripheral glaciers of Greenland and Antarctica) at monthly scale for the period extending from January 1948 to December 2016. Gridded annual time series of glacier area computed with GGM, as well as monthly time series of total (liquid plus solid) precipitation on glacier area from the atmospheric forcing were also used in this study. Glacier area data was required to adapt the land area fraction within WaterGAP cells. In addition, precipitation on glacier area was required to calculate glacier runoff (see Section 3.3 for more details). Note that, to produce the gridded GGM data sets, each glacier was assigned to the grid cell that contains its center point (as given in the RGI version 6.0) even if, in reality, the glacier stretches across several grid cells. The data sets used in this study correspond to a simulation in which GGM was forced by the mean of an ensemble of seven global gridded atmospheric data sets (New et al., 2002; Saha et al., 2014; Compo et al., 2011; Dee et al., 2011; Kobayashi et al., 2015; Poli et al., 2016; Gelaro et al., 2017) data sets (New et al., 2000; Saha et al., 2010; Compo et al., 2011; Dee et al., 2011; Kobayashi et al., 2015; Poli et al., 2016; Gelaro et al., 2017; New et al., 2002). Note that choosing the ensemble mean over any of the individual atmospheric data sets allows reducing the uncertainty due to input climate forcing data.

**Deleted:** (New et al., 2002; Saha et al., 2014; Compo et al., 2011; Dee et al., 2011; Kobayashi et al., 2015; Poli et al., 2016; Gelaro et al., 2017) data sets (New et al., 2000; Saha et al., 2010; Compo et al., 2011; Dee et al., 2011; Kobayashi et al., 2015; Poli et al., 2016; Gelaro et al., 2017; New et al., 2002). Note that choosing the ensemble mean over any of the individual atmospheric data sets allows reducing the uncertainty due to input climate forcing data.

**Deleted:** data sets (New et al., 2000; Saha et al., 2010; Compo et al., 2011; Dee et al., 2011; Kobayashi et al., 2015; Poli et al., 2016; Gelaro et al., 2017; New et al., 2002). Note that choosing the ensemble mean over any of the individual atmospheric data sets allows reducing the uncertainty due to input climate forcing data.

**Deleted:** (New et al., 2000; Saha et al., 2010; Compo et al., 2011; Dee et al., 2011; Kobayashi et al., 2015; Poli et al., 2016; Gelaro et al., 2017; New et al., 2002). Note that choosing the ensemble mean over any of the individual atmospheric data sets allows reducing the uncertainty due to input climate forcing data.

**Deleted:** . Note that choosing the ensemble mean over any of the individual atmospheric data sets allows reducing the uncertainty due to input climate forcing data.



### 2.2.2 Modelled LGWSA

400 GGM computes glacier mass change at the scale of individual glaciers, however for this study the data were provided on a rectangular 0.5° by 0.5° grid covering the entire globe (excluding ice sheet peripheral glaciers). Gridded annual time series of glacier area computed with GGM, as well as monthly time series of total (liquid plus solid) precipitation on glacier area from the atmospheric forcing were also used in this study. Glacier area data was required to adapt the land area fraction within WaterGAP cells. In addition, precipitation on glacier area was required to calculate glacier runoff (Section 2.3.1).  
405 Note that, to produce the gridded GGM data sets, each glacier was assigned to the grid cell that contains its center point (as given in the RGI version 6.0) even if, in reality, the glacier stretches across several grid cells. Furthermore, we applied a number of pre-processing steps to the GGM gridded data in order to make it suitable as input data for WaterGAP (described in Section S1.1 of the supplementary information).

### 2.2.3 Glacier mass change from in situ observations

410 Time series of annual and seasonal glacier surface mass balance at the scale of individual glaciers derived from in situ observations from the “reference glaciers” sample of the World Glacier Monitoring Service (2017) were used to evaluate the performance of GGM. This constitutes a reliable and well-documented sample of globally distributed long-term observation series. By “seasonal”, we refer to the winter and summer seasons within a glacier mass balance year. During the winter (accumulation) season, the glacier tends to gain mass, while during the summer (melting) season, it tends to lose mass. A  
415 glacier was selected from the sample if 1) its observations corresponded to the entire glacier and not solely to sections of it, 2) it had a minimum of five years with observations for both summer and winter and 3) it was among the glaciers simulated by GGM. In total, 31 glaciers were selected (see Table S1 in the supplementary material).

### 2.2.4 GRACE-derived TWSA

420 Global time series of mass change over continents were derived from ITSG-Grace2018 (Mayer-Gürr et al., 2018) and GRACE Release 6 (CSR, GFZ, JPL) quasi-monthly Level-2 gravity field solutions by means of global spherical harmonic (SH) coefficients. We further processed the SH solutions in order to derive global grids of surface mass change. Monthly resolved solutions expanded up to degree and order 60 were chosen for the lower noise level compared to higher resolved solutions. We substituted Degree-1 (geocenter motion) coefficients following the approaches of Swenson et al. (2008) and Bergmann-Wolf et al. (2014), and  $C_{2,0}$  (Earth’s oblateness) coefficients after Cheng et al. (2013), respectively. Gravity  
425 changes related to glacial isostatic adjustment (GIA) were accounted for using GIA modelling results from Caron et al. (2018). Furthermore, we excluded areas with considerable mass redistribution related to the 2004/2005 Sumatra/Nias- and the 2011 Tōhoku earthquakes from the integration. As we preferred unconstrained SH solutions over a-priori regularized mascon products, we corrected for the coastal leakage effect from continent to ocean by expanding the initial land–water mask by a 300 km buffer onto the ocean. The gravity field over this buffer area contains signal from both land and ocean. In  
430 order to counteract this superposition, we subtracted the monthly mean value of the buffered Global Ocean surface-density

change (obtained from the corresponding SH solution) multiplied by the fractional ocean area of the buffer cells, respectively. Here, we assume the actual mean ocean mass change over the buffer to equal the global mean ocean mass change.

The resulting integrated and corrected signal was attributed to the initial land–water mask (i.e. the one used by WaterGAP) area and represents the global (Antarctica and Greenland excluded) continental mass change from hydrology and glaciers, since it is impossible for GRACE to make the distinction. The GRACE trend uncertainty is a  $1\sigma$  standard uncertainty and was assessed from several components in the time series processing that have a significant impact on the trend. It comprises uncertainty due to leakage, degree-1 and  $C_{2,0}$  replacements, and GIA corrections. The combined trend uncertainty is the root sum squared of these components and is identical for all GRACE time series.

## 2.3 Methods

### 2.3.1 Integration of GGM glacier data into WaterGAP

Each WaterGAP grid cell has a continental area ( $A_C$ ), i.e. the part of the grid cell that is not ocean.  $A_C$  consists of spatially and temporally varying fractions of land area ( $A_L$ ) (where precipitation infiltrates into the soil) and areas of surface water bodies if there are lakes, wetlands and/or reservoirs. If a fraction of  $A_L$  is covered by glacier according to GGM, then the simulation of hydrological processes (evapotranspiration, runoff generation etc.) is restricted, in the integrated WaterGAP version, to the glacier-free fraction of  $A_L$ . In the gridded glacier area ( $A_{LG}$ ) data set, the entire area of each glacier is assigned to the cell where the center of the glacier is located. However, in reality, some glaciers are spread over more than one cell; this means that sometimes input  $A_{LG}$  is larger than  $A_C$ . In such cases,  $A_{LG}$  is set to be equal to  $A_C$  to avoid inconsistencies. As a result of this adaptation, we systematically neglect 10 to 11% (depending on the year) of the global  $A_{LG}$  over the period 1948–2016 (but not the pertaining LGWSA). The adapted  $A_{LG}$  is then used to adjust  $A_L$  (Figure 1). In the initial simulation year ( $yr = 1$ ),  $A_L$  (which is equal to the initial  $A_L$  of the standard WaterGAP) is reduced by  $A_{LG}$ . In the following years,  $A_L$  is adapted by the glacier area change ( $\Delta A_{LG}$ ), which can be either positive or negative (i.e. area increase or decrease). Areas of surface water bodies are not adapted according to  $A_{LG}$ . Glacier mass change ( $dLGWS/dt$ ) computed by GGM is added, along with changes in the other storage compartments, to TWS change (Figure 1). We assume that the only ongoing hydrological process on  $A_{LG}$  is runoff generation from precipitation on the glacier ( $P_{LG}$ ) and LGWS change ( $dLGWS/dt$ ). The generated runoff is hereafter called glacier runoff ( $R_{LG}$ ) and calculated according to Eq. (3):

$$R_{LG} = P_{LG} - dLGWS/dt \quad (3)$$

If daily increase in glacier mass is larger than daily  $P_{LG}$ ,  $R_{LG}$  is set to zero.  $R_{LG}$  is added to the cell's fast runoff, which partly flows directly into the river and partly into the other surface water bodies (Figure 1). We assume that  $R_{LG}$  does not recharge the soil and groundwater storages. The thus enhanced WaterGAP, the "integrated" WaterGAP, is capable of actually simulating TWSA on the continents (as observable by GRACE), while the standard WaterGAP neglects the impact of glaciers on TWSA.

Deleted: SWB

Deleted: SWB

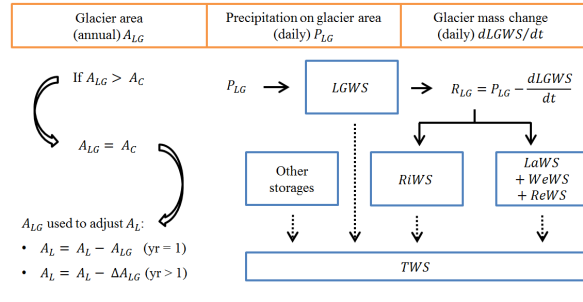


**Figure 1:** Schematic of integration of glacier data from GGM into WaterGAP at grid cell scale. Glacier data sets are represented by orange boxes. Blue boxes represent water storage compartments in WaterGAP (for acronyms, refer to Eq. 2). Full arrows represent water flows and dotted arrows indicate that the sum of changes in individual storages equals TWS change. See text for details and abbreviations.

### 2.3.2 Model experiments

Two model versions, standard WaterGAP (Wg\_std) and integrated WaterGAP (Wg\_gl), were run under four different model configurations or modes (Table 1).

**Table 1:** Overview of model variants used in this study. The standard version of WaterGAP2.2d (Wg\_std) and a non-standard version which implicitly includes glaciers (Wg\_gl) were run under four types of model configuration (“anthropogenic”, “anthropogenic without reservoirs”, “anthropogenic without water abstraction” and “naturalized”), two climate forcings differing in terms of precipitation bias correction (based on GPCC or CRU), and two assumptions related to consumptive irrigation water use (“70% deficit” and “optimal”).

Model version	Model configuration	Precipitation bias correction	Consumptive irrigation water use	Model variant name	Number of model variants
Standard WaterGAP (Wg_std)	Anthropogenic	GPCC <sup>1</sup> / CRU <sup>2</sup>	70% deficit (irr70) / optimal (irr100)	WGHM_std_ant [PREC] [IRR]	4
Integrated WaterGAP (Wg_gl)	Anthropogenic	GPCC <sup>1</sup> / CRU <sup>2</sup>	70% deficit (irr70) / optimal (irr100)	WGHM_gl_ant [PREC] [IRR]	4
	Anthropogenic without reservoirs	GPCC <sup>1</sup> / CRU <sup>2</sup>	70% deficit (irr70) / optimal (irr100)	WGHM_gl_ant_nores [PREC] [IRR]	4
	Anthropogenic without water abstraction	GPCC <sup>1</sup> / CRU <sup>2</sup>	-	WGHM_gl_ant_noabs [PREC]	2
	Naturalized	GPCC <sup>1</sup> / CRU <sup>2</sup>	-	WGHM_gl_nat [PREC]	2

**Deleted:** In order to generate the monthly and annual TWSA time series used in this study, t...

**Moved (insertion) [12]**

**Moved (insertion) [9]**

**Moved (insertion) [10]**

**Deleted:** In anthropogenic mode (standard mode), the model takes into account both climate variability and anthropogenic variability, the latter referring to the effects of water impoundment in reservoirs and of human water abstraction. In naturalized mode, the model takes into account only climate variability; this means that reservoirs are not simulated at all (except for regulated lakes, which are treated as natural lakes) and water abstraction is neglected. By comparing outputs from anthropogenic and naturalized runs, it is possible to isolate the water storage change solely due to the human activities (Table 2). WaterGAP also allows performing runs that neglect reservoirs but take into account water abstraction, and vice-versa; these model variants are interesting for the purpose of isolating the effect of water impoundment in reservoirs from the effect of water abstraction (Table 2). Each combination of model version and model configuration was run under two climate forcings, WFDEI-GPCC and WFDEI-CRU.

Marzeion et al. (2012) compared in situ observations of glacier annual SMB (from the collections of the World Glacier Monitoring Service) to estimates obtained with GGM. The results showed a good correlation ( $r = 0.60$  for set of 3997 pairs of annual modelled and measured SMB) and from this it is concluded that GGM can reconstruct annual mass balances of unmeasured glaciers with reasonable accuracy. In this study, which focuses not only on the annual but also on the monthly scale, we investigated the performance of GGM at seasonal scale. By “seasonal”, we refer to the winter and summer seasons within a glacier mass balance year. During the winter (accumulation) season (October to March in the Northern hemisphere and April to September in the Southern hemisphere), the glacier tends to gain mass, while during the summer (melting) season (April to September in the Northern hemisphere and October to March in the Southern hemisphere), the glacier tends to lose mass. For the comparison, we used the estimates computed by GGM at the scale of individual glaciers. The observational data was selected from the “reference glaciers” sample of the World Glacier Monitoring Service (2017). This constitutes a reliable and well-documented sample of globally distributed long-term observation series. A glacier was selected from this sample if 1) its observations corresponded to the entire glacier and not solely to sections of it, 2) it had a minimum of five years with observations for both summer and winter and 3) it was among the glaciers simulated by GGM. In total, 31 glaciers worldwide were selected (see Table S1 in the supplementary material).

Each WaterGAP grid cell has a continental area ( $A_C$ ), the part of the grid cell that is not ocean. The continental area consists of spatially and temporally varying fractions of land area ( $A_L$ ) (where precipitation infiltrates into the soil) and areas of SWB if there are [4]

**Moved (insertion) [11]**

**Deleted:** Figure 1: Schematic of integration of glacier data from GGM into WaterGAP at grid cell scale. Glacier-related data sets are represented by orange boxes. Blue boxes represent water storage compartments in WaterGAP. Full arrows represent water flows and dotted arrows indicate that the sum of changes in individual storages equals TWS change. See text for details and abbreviations.

<sup>1</sup>Schneider et al. (2015). <sup>2</sup>Harris et al. (2014).

In anthropogenic mode (standard mode), the model takes into account both climate- and human-induced variability. In naturalized mode, the model takes into account only climate variability; reservoirs (except for regulated lakes, which are treated as natural lakes) and water abstraction are not simulated. By comparing outputs from anthropogenic and naturalized runs, it is possible to isolate the water storage change solely due to the human activities (Table 2). WaterGAP also allows performing runs that neglect reservoirs but take into account water abstraction, and vice-versa; these configurations can be used for isolating the effect of water impoundment in reservoirs from the effect of water abstraction (Table 2). Each combination of model version and model configuration was run under two climate forcings, WFDEI-GPCC and WFDEI-CRU.

In addition, we considered two different assumptions with respect to consumptive irrigation water use based on Döll et al. (2014). This flow is normally computed under the assumption that crops receive enough irrigation water to allow actual evapotranspiration to become equal to potential evapotranspiration (Döll et al., 2016). However, this is not always the case in regions affected by groundwater depletion, where farmers may use less water due to water scarcity. Groundwater depletion is defined as a long-term decline of hydraulic heads and groundwater storage. Using a former version of WaterGAP, Döll et al. (2014) identified groundwater depletion areas worldwide by selecting the grid cells characterized by 1) an average groundwater depletion of at least 5 mm yr<sup>-1</sup> over the period 1980–2009 and 2) an irrigation water abstraction volume of at least 5% of total water abstraction volume. In this study, we either assumed that consumptive irrigation water use is optimal (i.e. that it corresponds to 100% of water requirement) or that it is equal to 70% of optimal in these groundwater depletion areas (“optimal” and “70% deficit” irrigation variants in Table 1).

**Table 2:** Overview of how the TWSA mass budget components were calculated using the integrated WaterGAP variants. TWSA[ant], TWSA[nat], TWSA[ant\_nores] and TWSA[ant\_noabs] were computed under the ‘anthropogenic’, ‘naturalized’, ‘anthropogenic without reservoirs’ and ‘anthropogenic without water abstraction’ configurations, respectively. LGWSA remains unchanged.

Component	Computation	Model configuration(s) used
LWSA	TWSA[ant] – LGWSA	‘Anthropogenic’
LWSA <sub>clim</sub>	TWSA[nat] – LGWSA	‘Naturalized’
LWSA <sub>hum</sub>	TWSA[ant] – TWSA[nat]	‘Anthropogenic’ and ‘naturalized’
LWSA <sub>res</sub>	TWSA[ant] – TWSA[ant_nores]	‘Anthropogenic’ and ‘anthropogenic without reservoirs’
LWSA <sub>abs</sub>	TWSA[ant] – TWSA[ant_noabs]	‘Anthropogenic’ and ‘anthropogenic without water abstraction’

**Deleted: Global hydrological model!**

General structure<sup>1</sup>

We used the latest version of the GHM WaterGAP, WaterGAP2.2d. WaterGAP simulates both human water use as well as daily water flows and water storages (or anomalies) on a 0.5° by 0.5° grid (55 km by 55 km at equator and ~3000 km<sup>2</sup> grid cell) covering the global continental area except for Antarctica (see Fig. 1 in Döll et al., 2014). We ignored model outputs over the grid cells corresponding to Greenland because this study focuses on anomalies over continental area different from the ice sheets. Streamflow is laterally routed through the stream network derived from the global drainage direction map DDM30 (Döll and Lehner, 2002) until it reaches the ocean or an inland sink. The model is calibrated against observations of mean annual streamflow at 1319 gauging stations (Müller Schmied et al., 2014).<sup>2</sup>

The model requires daily climatological input data sets of precipitation (rainfall and snowfall), near-surface air temperature, and<sup>3</sup>

**Deleted:** (Lehner et al., 2011). The simulation of reservoir operation is based on the generic algorithm of Hanasaki et al. (2006), which distinguishes between irrigation and non-irrigation reservoirs.<sup>4</sup>

**Moved up [7]:** WaterGAP represents the transport of water on among a series of individual water storage compartments (see Figure 1 in Döll et al., 2014). It includes all continental water storage

**Deleted:** (see Figure 1 in Döll et al., 2014). It includes all continental water storage compartments except for glaciers. Thus, glacierized areas are treated as non-glacierized areas. LWSA, which<sup>5</sup>

**Moved up [9]:** Marzeion et al. (2012) compared in situ observations of glacier annual SMB (from the collections of the World Glacier Monitoring Service) to estimates obtained with GGM.

**Moved up [10]:** Each WaterGAP grid cell has a continental area grid cell that is not ocean. The continental area consists of spatially and temporally varying fractions of land area (A<sub>L</sub>) (where

**Deleted:** Marzeion et al. (2012). The model computes mass changes of individual glaciers for the whole globe. It combines a glacier SMB model, following an empirically based temperature, ...<sup>6</sup>

**Moved up [8]:** GGM computes glacier mass change at the scale of glaciers worldwide. In the framework of this study, the data were provided on a rectangular 0.5° by 0.5° grid (for consistency with

**Deleted:** <#>Pre-processing of gridded GGM output data<sup>7</sup>  
We applied a number of pre-processing steps to the GGM gridded data in order to make it suitable as input data for WaterGAP. For<sup>8</sup>

**Moved up [11]:** Figure 1: Schematic of integration of glacier data from GGM into WaterGAP at grid cell scale. Glacier-related data sets are represented by orange boxes. Blue boxes represent water stor<sup>9</sup>

**Deleted:** (New et al., 2000; Saha et al., 2010; Compo et al., 2011; Dee et al., 2011; Kobayashi et al., 2015; Poli et al., 2016; Gelaro et al., 2017). Note that choosing the ensemble mean over any of the. [9]

**Deleted:** ¶  
¶  
... [12]

**Deleted:** ¶  
Model version ... [13]

**Deleted:** Schneider et al. (2015). <sup>2</sup>Harris et al. (2014).<sup>3</sup>  
In addition, inspired by the study of Döll et al. (2014), we considered two different assumptions with respect to consumptive irrigation ... [14]

### 3. Results

#### 3.1 Model evaluation

To evaluate the performance of GGM, simulated glacier mass changes of individual glaciers were compared to glacier observations (Section 3.1.1). Then, global mean TWSA simulated by WaterGAP with and without integration of GGM output was compared to GRACE observations (Section 3.1.2).

##### 3.1.1 Comparison of observed and simulated annual and seasonal glacier mass changes

Comparison of observed average annual glacier mass changes for 31 glaciers with mostly decades of observations (Table S1) confirms the conclusion of Marzeion et al. (2012) that GGM is able to simulate well annual glacier mass changes. This study reveals that both average winter accumulation and summer melting are simulated reasonably too, but worse than the average annual mass changes, with Nash–Sutcliffe efficiencies NSE (Eq. (1), Nash and Sutcliffe, 1970) and correlation coefficients  $r$  being slightly lower than for the annual values (Figure 2). We also quantified, for each glacier, the fit between simulated and observed time series of winter and summer mass changes (two values per year times the number of years with observations). Approximately three-quarters of the glaciers have a NSE higher than 0.70 (Table S1), indicating a good model performance at the seasonal time scale even though GGM was only tuned with respect to the annual values. Only two glaciers, the “Devon Ice Cap NW” and the “Vernagtferner”, show a negative NSE. The first is a marine-terminating ice cap where calving processes that are not modelled explicitly by GGM occur.

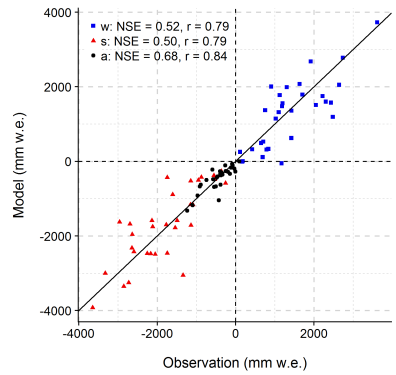


**Figure 2:** Correlation between observed and modelled average annual, winter and summer glacier mass change. Observations were taken from the collections of the World Glacier Monitoring Service (31 glaciers included). Model results were obtained with the global glacier

Deleted: Model evaluation

Moved (insertion) [1]

Deleted: quality

model of Marzeion et al. (2012). Nash–Sutcliffe efficiency (NSE) and correlation coefficient ( $r$ ) values correspond to average annual (a), winter (w) and summer (s) mass changes. Millimetres of water equivalent (mm w.e.) are relative to glacier area.

### 3.1.2 Comparison of observed and simulated global mean TWSA during January 2003 to August 2016

Figure 3a presents time series of the ensemble of monthly TWSA simulated by the standard (without glaciers) and the integrated (with glaciers) WaterGAP versions compared to GRACE observations. The NSE- and  $r$ -values shown in the figure were computed for the mean of the GRACE ensemble (consisting of four solutions) and the means of the Wg\_std and Wg\_gl ensembles (each ensemble consisting of the four anthropogenic variants, see Table 1). For both Wg\_std and Wg\_gl, there is a remarkably good fit between the modelled and the GRACE ensemble means in terms of NSE (0.85, 0.87) and  $r$  (0.92, 0.95), both of which rather reflect the good fit of seasonal variability than of the trend. The fit is slightly better with Wg\_gl, not only in terms of ensemble mean but also if we consider the NSE- and  $r$ -values obtained by comparing each individual GRACE solution to each individual WaterGAP solution (see Figure S2 in the supplementary material). With NSE around 0.80 during the period January 2003 to December 2008, the fit is worse during the first six evaluation years than during the following period until August 2016 (Figure 3a). Note however that the period from 2011 onward contains more gaps in the GRACE data. Glaciers lead to a much stronger decreasing TWSA trend over the period considered. Monthly time series of LGWSA from GGM have a small seasonal variability and an almost linear decreasing trend (Figure 3b). When adding LGWSA to the LWSA computed by Wg\_std (Wg\_std+GGM), the resulting time series of global mean values (purple ensemble in Fig. 3b) is indistinguishable from the TWSA time series computed by Wg\_gl (green ensemble in Fig. 3a).

Moved (insertion) [2]

Deleted: under anthropogenic conditions

Deleted: ensemble mean

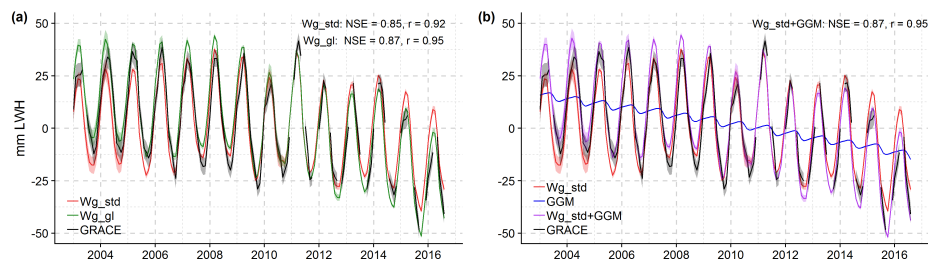


Figure 3: Global mean monthly TWSA from GRACE observations and from different modelling approaches, January 2003 to August 2016. (a) TWSA from GRACE ensemble, LWSA from standard WaterGAP (Wg\_std) in anthropogenic mode ensemble (Wg\_std ant CRU irr100, Wg\_std ant CRU irr70, Wg\_std ant GPCC irr100 and Wg\_std ant GPCC irr70 in Table 1) and TWSA from integrated WaterGAP (Wg\_gl) in anthropogenic mode ensemble (Wg\_gl ant CRU irr100, Wg\_gl ant CRU irr70, Wg\_gl ant GPCC irr100 and Wg\_gl ant GPCC irr70 in Table 1). (b) TWSA from GRACE ensemble, LWSA from Wg\_std ensemble as in (a), LGWSA from GGM and TWSA obtained by adding anomalies from Wg\_std ensemble and GGM (Wg\_std+GGM). For each ensemble, the curve represents the ensemble mean and the shaded area around the curve represents either the uncertainty range (GRACE)

765 or the ensemble range ( $Wg\_std$ ,  $Wg\_gl$  and  $Wg\_std+GGM$ ). Nash–Sutcliffe efficiency (NSE) and correlation coefficient ( $r$ ) obtained by comparing GRACE and model ensemble means are provided. Anomalies are relative to the mean over January 2006 to December 2015. Millimetres of land water height (mm LWH) are relative to the global continental area without the ice sheets ( $132.3 \cdot 10^6 \text{ km}^2$ ).

770 To evaluate WaterGAP performance separately regarding its simulation of seasonality, trend and interannual variability, the original monthly TWSA time series (Figure 3a) were decomposed (based on harmonic analysis) into de-trended, de-seasonalized and residual TWSA (Figure 4). Regarding seasonality, there is a remarkably good fit to GRACE with both  $Wg\_std$  and  $Wg\_gl$ : the seasonal amplitude and phase are very well reproduced by the models, even though for some years (e.g. 2003, 2004, 2011, 2014) there seems to be a slight phase shift of approximately one month (Figures 4a–b). The indicators show that the fit is very good with the two models and only slightly better for  $Wg\_gl$ , reflecting the small contribution of glaciers to the seasonal variation of global mean TWSA (NSE of 0.89 instead of 0.88 due to slightly increasing seasonal amplitude). The de-seasonalized time series show the strong impact of including glaciers into WaterGAP.  $Wg\_gl$  can follow the negative trend of TWSA observed by GRACE much better than  $Wg\_std$  (Figures 4c–d), and performance indicators are significantly higher (NSE improves from 0.65 to 0.74 and  $r$  from 0.85 to 0.93). However, the GRACE signal is overestimated before 2011 (in particular during 2007–2009) and in 2016, and underestimated in 2011. The overestimation during 2007–2009 may be partly due to a drought period in the Near East when a large number of new groundwater wells were drilled in this region, which is not taken into account in WaterGAP simulations of groundwater vs. surface water use (Döll et al., 2014). The residual signal present in the original time series (Figures 4e–f), which includes the interannual variability, is very similar for the two models, which suggests that GGM does not contribute to the residual. With an NSE of 0.57, the fit of the residuals and thus simulation of interannual variability is relatively good but worse than for de-trended and de-seasonalized time series. The discrepancies to the GRACE signal follow the same pattern as in Figures 4c–d. However, the fit to GRACE before 2007 is better than in the latter.

785 Linear trends are very sensitive to the selected time period and individual values. While the de-seasonalized TWSA from  $Wg\_gl$  fits reasonably well overall to GRACE observations (Fig. 4d),  $Wg\_gl$  considerably overestimates the trend determined for the time period January 2003 to August 2016, if averaged over the four ensemble members, by about 30% (Table 3).  $Wg\_std$  variants underestimate the positive contribution to ocean mass change by about 50%. Thus, the TWSA trend computed by integrating GGM output into WaterGAP results in a better estimation of the GRACE trend than if glaciers are neglected. Assuming 70% deficit irrigation and utilizing GPCC precipitation, the simulated trend value of 1.05 mm SLE  $\text{yr}^{-1}$  is within the uncertainty bounds of the GRACE solutions (Table 3). The trend gets larger with optimal irrigation and CRU precipitation, which is mainly due to the larger TWSA values during the period 2003–2004 (Fig. 4d). The absolute difference between the two irrigation variants (0.11 to 0.12 mm SLE  $\text{yr}^{-1}$ ) is practically equal to the absolute difference between the two precipitation forcings (0.11 to 0.13 mm SLE  $\text{yr}^{-1}$ ); this means that, over this period, the trend is equally affected by the choice of irrigation variant than by the choice of precipitation forcing. The GRACE ensemble range is approximately 5 times smaller than the range of the  $Wg\_std$  and  $Wg\_gl$  ensembles. This is partly due to the choice of

Moved (insertion) [3]

Deleted: -

Deleted: (Figures 4a and 4b)

Deleted: (Figures 4c and 4d)

Deleted: (Figures 4e and 4f)

Deleted: and 4

Deleted: The de-seasonalized time series show the strong impact of including glaciers into WaterGAP.  $Wg\_gl$  can follow the decrease of TWSA observed by GRACE much better than  $Wg\_std$  (Figures 4c and 4d), and performance indicators are significantly higher (NSE improves from 0.65 to 0.74 and  $r$  from 0.85 to 0.93). ¶

GRACE solutions; although coming from different processing centres, they were all corrected using the same GIA model (Caron et al., 2018). The trend-spread owing to possible GIA models is reflected in the given standard uncertainty. The GIA model choice is the main contributor to uncertainty besides the GRACE degree-1 correction.

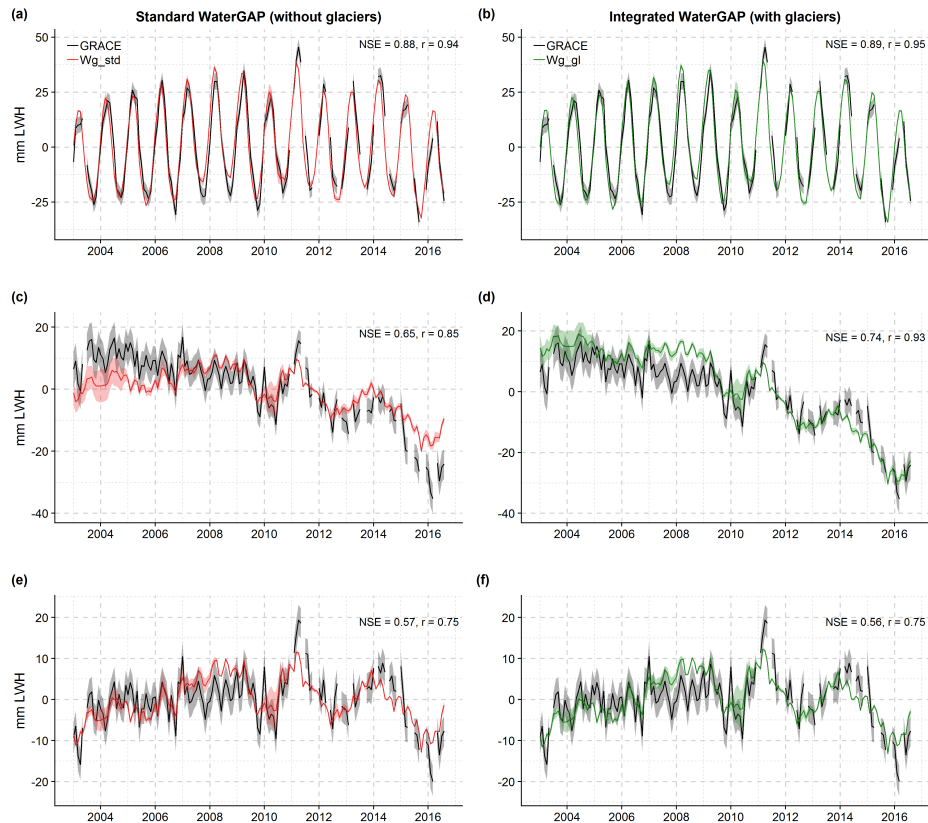


**Figure 4:** Temporal components of global mean monthly TWSA from GRACE observations and from two versions of WaterGAP2.2d, January 2003 to August 2016. GRACE ensemble, standard WaterGAP ( $Wg\_std$ ) ensemble (a, c, e) and integrated WaterGAP ( $Wg\_gl$ ) ensemble (b, d, f). (a,b) De-trended anomalies. (c,d) De-seasonalized anomalies (correspond to linear and non-linear long-term variability). (e,f) Residual anomalies obtained by removing linear trend and seasonality (correspond to non-linear inter-annual variability). For each

**Moved up [1]:** To evaluate the quality of GGM, simulated glacier individual glaciers were compared to glacier observations. Then, global mean TWSA simulated by WaterGAP with and without integration of GGM output was compared to GRACE observations. **Comparison of observed and simulated annual and seasonal glacier mass changes**

Comparison of observed average annual glacier mass changes for 31 glaciers with mostly decades of observations (Table S1) confirm the conclusion of Marzeion et al. (2012) that GGM is able to simulate well annual glacier mass changes. This study reveals that both winter accumulation and summer melting is simulated reasonably, too, but worse than the annual mass changes, with Nash-Sutcliffe efficiencies NSE (Eq. (1), Nash and Sutcliffe, 1970) and correlation coefficients  $r$  being slightly lower than for the annual values (Figure 2). We also quantified, for each glacier, the fit between simulated and observed time series of winter and summer mass changes (two values per year times the number of years with observations). Approximately three-quarters of the glaciers have a NSE higher than 0.70 (Table S1), indicating a good model performance at the seasonal time scale even though GGM was only tuned with respect to the annual values. Only two glaciers, the “Devon Ice Cap NW” and the “Vernagtferner”,

**Deleted:**

To evaluate the quality of GGM, simulated glacier mass changes of individual glaciers were compared to glacier observations. Then, global mean TWSA simulated by WaterGAP with and without integration of GGM output was compared to GRACE observations.

**Comparison of observed and simulated annual and seasonal glacier mass changes**  
Comparison of observed average annual glacier mass changes for 31 glaciers with mostly decades of observations (Table S1) confirm the conclusion of Marzeion et al. (2012) that GGM is able to simulate

**Moved up [2]:** Figure 3a presents time series of the ensemble of simulated by the standard (without glaciers) and the integrated (with glaciers) WaterGAP versions compared to GRACE observations. The NSE- and  $r$ -values shown in the figure were computed for the mean of the GRACE ensemble (consisting of four solutions) and the means of the  $Wg\_std$  and  $Wg\_gl$  ensembles (each ensemble consisting of the four variants under anthropogenic conditions, see Table 1). For both  $Wg\_std$  and  $Wg\_gl$ , there is a remarkably good fit between the modelled ensemble mean and the GRACE ensemble mean in terms of NSE (0.85, 0.87) and  $r$  (0.92, 0.95), both of which rather reflect the

**Deleted: Figure 3:** Global mean monthly TWSA from GRACE observations and from different modelling approaches, January 2003 to August 2016. (a) TWSA from GRACE ensemble, LWSA from standard WaterGAP ( $Wg\_std$ ) in anthropogenic mode ensemble ( $Wg\_std\_ant\_CRU\_irr100$ ,  $Wg\_std\_ant\_CRU\_irr70$ ,  $Wg\_std\_ant\_GPCC\_irr100$  and  $Wg\_std\_ant\_GPCC\_irr70$  in Table 1) and TWSA from integrated WaterGAP ( $Wg\_gl$ ) in anthropogenic mode ensemble ( $Wg\_gl\_ant\_CRU\_irr100$ ,  $Wg\_gl\_ant\_CRU\_irr70$ ,  $Wg\_gl\_ant\_GPCC\_irr100$  and  $Wg\_gl\_ant\_GPCC\_irr70$  in Table 1)

**Moved up [3]:** To evaluate WaterGAP performance separately regarding its simulation of seasonality, trend and inter-annual variability, the original monthly TWSA time series (Figure 3a) were decomposed (based on harmonic analysis) into de-trended (Figures 4a and 4b), de-seasonalized (Figures 4c and 4d) and residual (Figures 4e and 4f) TWSA. Regarding seasonality, there is a remarkably good fit to GRACE with both  $Wg\_std$  and  $Wg\_gl$ ; the seasonal amplitude and phase are very well reproduced by the models, even though for some years (e.g. 2003, 2004, 2011, 2014) there seems to be a slight

**Deleted:**



5990 ensemble, the curve represents the ensemble mean and the shaded area around the curve represents either the uncertainty range (GRACE)  
 or the ensemble range (Wg\_std and Wg\_gl). Nash-Sutcliffe efficiency (NSE) and correlation coefficient (r) obtained by comparing  
 GRACE and model ensemble means are provided. Anomalies are relative to the mean over January 2006 to December 2015 and given in  
 millimetres of land water height (mm LWH).

5995 Overall, we infer that integration of glacier model output into WaterGAP results in a better fit to GRACE in terms of linear  
 trend, NSE and r for de-seasonalized time series while simulated seasonality is barely improved. Seasonal variations of mean  
 global TWSA are simulated very well with Wg\_gl compared to GRACE observations, interannual variability is captured to a  
 certain extent, and the linear trend is overestimated. The overall fit of the monthly time series of global mean TWSA to  
 GRACE (Figure 3a) is remarkably good (NSE = 0.87, r = 0.95). Together with the positive evaluation of the glacier model  
 results, this gives us confidence that our modelling approach can be used to reconstruct TWSA and thus the water mass  
 3000 transfer from the continents to the oceans for the time period before GRACE.

5005 **Table 3: Linear trends of TWSA** from GRACE observations and from WaterGAP2.2d, January 2003 to August 2016. Model estimates  
 correspond to individual solutions of standard WaterGAP (Wg\_std) and integrated WaterGAP (Wg\_gl) ensembles. GRACE-derived  
 estimates correspond to SH solutions from four processing centres (CSR, GFZ, ITSG and JPL). Trends were calculated according to the  
 linear least squares regression method. Negative trends (mass loss) over the continents, expressed in millimetres of land water height (mm  
 LWH, relative to the global continental area without the ice sheets  $132.3 \cdot 10^6 \text{ km}^2$ ), translate to positive trends (mass gain) over the oceans,  
 expressed in millimetres of sea level equivalent (mm SLE, relative to the global ocean area  $361.0 \cdot 10^6 \text{ km}^2$ ).

Variant	Trend		Average of individual trends		
	mm LWH yr <sup>-1</sup>	mm SLE yr <sup>-1</sup>	mm LWH yr <sup>-1</sup>	mm SLE yr <sup>-1</sup>	
Wg_std	ant_GPCC_irr70	-0.78	0.29	-1.12	0.41
	ant_GPCC_irr100	-1.12	0.41		
	ant_CRU_irr70	-1.13	0.42		
	ant_CRU_irr100	-1.45	0.53		
Wg_gl	ant_GPCC_irr70	-2.86	1.05	-3.18	1.17
	ant_GPCC_irr100	-3.19	1.17		
	ant_CRU_irr70	-3.18	1.16		
	ant_CRU_irr100	-3.50	1.28		
GRACE	CSR_rl06sh	-2.37 ± 0.55	0.87 ± 0.20	-2.37 ± 0.55	0.87 ± 0.20
	GFZ_rl06sh	-2.39 ± 0.55	0.87 ± 0.20		
	ITSG_2018	-2.29 ± 0.55	0.84 ± 0.20		
	JPL_rl06sh	-2.43 ± 0.55	0.89 ± 0.20		

### 3.2 Global water transfer from continents to oceans over the period 1948–2016

#### 3.2.1 Contribution of total continental water storage (TWSA)

**Deleted:** minimum and maximum values

**Deleted:** the period

**Deleted:** However, the GRACE signal is overestimated before 2011 (in particular from 2007–2009) and in 2016, and underestimated in 2011. The overestimation from 2007–2009 may be partly due to a drought period in the Near East when a large number of new groundwater wells were drilled in this region, which is not taken into account in WaterGAP simulations of groundwater vs. surface water use (Döll et al., 2014). The residual signal present in the original time series (Figures 4e and 4f), which includes the inter-annual variability, is very similar for the two models, which suggests that GGM does not contribute to the residual. The fit of the residuals and thus simulation of inter-annual variability is relatively good but worse than for de-trended and de-seasonalized time series. The discrepancies to the GRACE signal follow the same pattern as in Figures 4c and 4d. However, the fit to GRACE before 2007 is better than in the latter.

Linear trends are very sensitive to the selected time period and individual values. While the de-seasonalized TWSA from Wg\_gl fits reasonably well overall to GRACE observations (Fig. 4d), Wg\_gl considerably overestimates the trend determined for the time period January 2003 to August 2016, if averaged over the four ensemble members, by about 30% (Table 3). Wg\_std variants underestimate the positive contribution to OMC by about 50%. Thus, the TWSA trend computed by integrating GGM output into WaterGAP results in a better estimation of the GRACE trend than if glaciers are neglected. Assuming 70% deficit irrigation and utilizing GPCC precipitation, the simulated trend value of 1.05 mm SLE yr<sup>-1</sup> is within the uncertainty bounds of the GRACE solutions (Table 3). The trend gets larger with optimal irrigation and CRU precipitation, which is mainly due to the larger TWSA values during the period 2003–2004 (Figure 4d). The absolute difference between the two irrigation variants (0.11 to 0.12 mm SLE yr<sup>-1</sup>) is in accordance with the absolute difference between the two precipitation forcings (0.11 to 0.13 mm SLE yr<sup>-1</sup>); this means that, over this period, the trend is equally affected by the choice of irrigation variant than by the choice of precipitation forcing. The GRACE ensemble range is approximately 5 times smaller than the range of the Wg\_std and Wg\_gl ensembles. This is partly due to the choice of the GRACE solutions; although coming from different processing centers, they were all corrected using the same GIA model (Caron et al., 2018). The trend-spread owing to possible GIA models is reflected in the given standard uncertainty. The GIA model choice is the main contributor to uncertainty besides the GRACE degree-1 correction.

**Deleted:** -

**Deleted:** ¶

**Deleted:** TWSA

Annual time series of global mean water storage anomalies over 1948–2016 were computed with integrated WaterGAP in anthropogenic mode (Figure 5a). The continents lost between 93–111 mm LWH to the oceans between 1948 and 2016, equivalent to an ocean water mass increase of 34–41 mm SLE. Sea-level rise is less pronounced in case of less than optimal irrigation in groundwater depletion areas (variant *irr70*, see Fig. 5b). While the 2003–2016 trends are equally affected by the precipitation data set and the irrigation assumption (Table 3), the 1948–2016 trends are much more strongly affected by the irrigation assumption than the applied precipitation data set (Fig. 5b). Continental water mass losses have been accelerating over time (see Table 4 and Table S2 in the supplementary material) so that the 2003–2016 trends are approximately 6 times larger than the 1948–1975 trends.

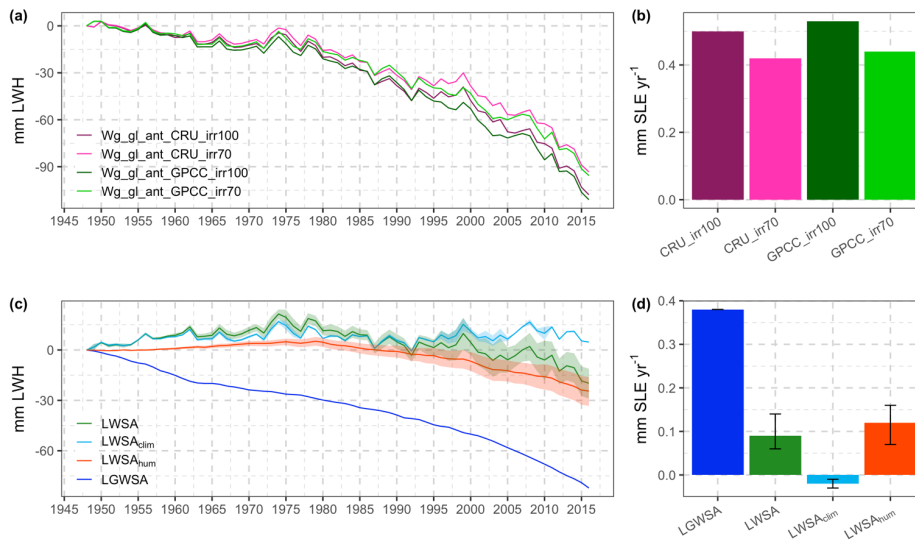


**Figure 5:** Global annual TWSA and individual contributions, 1958 to 2016. TWSA were computed with four variants of integrated WaterGAP in anthropogenic mode (Table 1) and disaggregated into anomalies of land glacier water storage (LGWSA) and land water storage (LWSA). LWSA were further disaggregated into anomalies of climate-driven land water storage (LWSA<sub>clim</sub>) and human-driven land water storage (LWSA<sub>hum</sub>). (a) Time series of TWSA and (b) corresponding linear trends of contribution of TWSA to ocean mass change over 1948–2016. (c) Time series of LWSA, LWSA<sub>clim</sub>, LWSA<sub>hum</sub> and LGWSA (for each ensemble, the curve represents the ensemble mean and the shaded area around the curve represents the ensemble range) and (d) corresponding linear trends (ensemble ranges are represented as errorbars). Anomalies are relative to the year 1948 and given in millimetres of land water height (mm LWH). Trends are

**Deleted:** ¶  
 <#>Global water transfer from continents to oceans over the period 1948–2016¶  
**Deleted:** the period  
**Deleted:** calculated by the four  
**Deleted:** variants with different precipitation inputs and irrigation water assumptions ...  
**Deleted:** which is  
**Deleted:** LR  
**Deleted:** also  
**Deleted:** Table 4  
**Deleted:** Table 4  
**Deleted:** 5

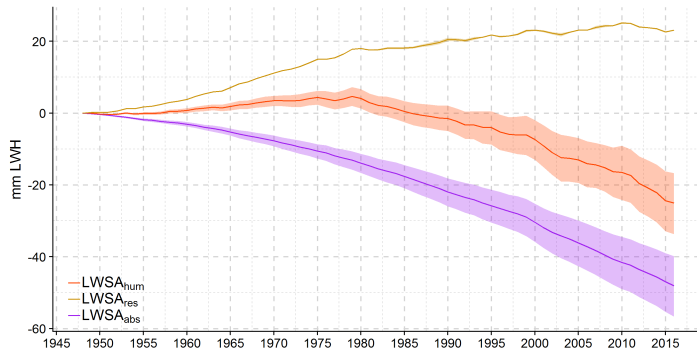
given in millimetres of sea level equivalent per year (mm SLE yr<sup>-1</sup>); positive trends translate to ocean mass gain, whereas negative trends translate to ocean mass loss.

### 3.2.2 Contributions of glaciers (LGWSA), climate-driven land water storage (LWSA<sub>clim</sub>) and human-driven land water storage (LWSA<sub>hum</sub>)

Simulated TWSA (Fig. 5a-b) was disaggregated into its individual components LGWSA, LWSA<sub>clim</sub> and LWSA<sub>hum</sub> (Fig. 5c-d) using the results of the different Wg<sub>gl</sub> model variants (Tables 1 and 2). Glacier mass loss is the dominant component of the TWSA mass budget (Fig. 5c-d), with LGWSA accounting for 81% of the cumulated water mass loss from continents to oceans over 1948–2016. Overall, the contribution of LWSA to ocean mass change, which is dominated by its human-driven component (Fig. 5d), is also positive, representing 19% of the cumulated water mass loss from continents. Interannual variability of LWSA stems from its climate-driven component (Fig. 5c). Trends of TWSA, LGWSA, LWSA, LWSA<sub>clim</sub> and LWSA<sub>hum</sub> show an acceleration of continental water mass loss over time (Table 4). However, note that LWSA<sub>clim</sub> and LWSA<sub>hum</sub> exhibit negative contributions to ocean mass change over the period 1948–1975, adding some water to the continents due to climate and human activities.

### 3.2.3 Contributions of reservoirs (LWSA<sub>res</sub>) and water abstraction (LWSA<sub>abs</sub>)

LWSA<sub>hum</sub> can be disaggregated into changes due to reservoir construction and operation (LWSA<sub>res</sub>) and changes due to human water abstraction (LWSA<sub>abs</sub>). Between 1948 and 2016, the continents gained approximately 22 mm LWH (i.e. 8 mm SLE) due to water impoundment in reservoirs, and lost between 40–57 mm LWH (i.e. 15–21 mm SLE) due to water abstraction for human water use, resulting in an overall positive contribution of LWSA<sub>hum</sub> to ocean mass change (Figures 5d and 6).



- Deleted: [17]
- Deleted: Figure 5: Global annual TWSA and individual ... [18]
- Deleted: LGWSA
- Deleted: LWSA
- Deleted: LWSA to TWSA
- Deleted: ure
- Deleted: ure
- Deleted: b
- Deleted: by
- Deleted: ure
- Deleted: b
- Deleted: The o
- Deleted:
- Deleted: ure
- Deleted: b
- Deleted: (
- Deleted: )
- Deleted: -
- Deleted: ure
- Deleted: b
- Deleted: 5
- Deleted: OMC
- Deleted: to human-driven LWSA
- Deleted: OMC

**Figure 6:** Global mean annual human-driven LWSA and individual contributions, 1948 to 2016. Human-driven LWSA ( $LWSA_{hum}$ , as in Figure 5c) are disaggregated into anomalies due to reservoir operation ( $LWSA_{res}$ ) and water abstraction ( $LWSA_{abs}$ ). Anomalies are relative to the year 1948 and given in millimetres of land water height (mm LWH).

However, continental water mass gain due to  $LWSA_{res}$  more than compensated mass losses due to  $LWSA_{abs}$  before 1980, when intensive reservoir construction led to a stronger increase of impounded water mass than afterwards (Figure 6). Trends of  $LWSA_{res}$  show a deceleration of continental mass gain due to water impoundment in reservoirs over time, whereas trends of  $LWSA_{abs}$  show an acceleration of continental mass loss due to water abstraction (Table 4).

**Table 4:** Linear trends of contribution of TWSA, LGWSA, LWSA,  $LWSA_{clim}$ ,  $LWSA_{hum}$ ,  $LWSA_{res}$ , and  $LWSA_{abs}$ , to ocean mass change over 1948–1975, 1976–2002 and 2003–2016. Positive trends translate to ocean mass gain, whereas negative trends translate to ocean mass loss. Ensemble ranges are given in parentheses. Estimates are given in millimetres of sea level equivalent per year ( $mm\ SLE\ yr^{-1}$ ).

Component	Linear trend $mm\ SLE\ yr^{-1}$		
	1948–1975	1976–2002	2003–2016
Total water storage anomaly (TWSA)	0.18 (0.13 to 0.23)	0.58 (0.49 to 0.66)	1.18 (1.06 to 1.30)
Lang glacier water storage anomaly (LGWSA)	0.38	0.37	0.77
Land water storage anomaly (LWSA)	-0.20 (-0.25 to -0.15)	0.21 (0.12 to 0.29)	0.41 (0.29 to 0.52)
Climate-driven land water storage anomaly ( $LWSA_{clim}$ )	-0.13 (-0.15 to -0.10)	0.01 (-0.02 to 0.04)	0.04 (-0.03 to 0.10)
Human-driven land water storage anomaly ( $LWSA_{hum}$ )	-0.08 (-0.10 to -0.05)	0.19 (0.14 to 0.25)	0.37 (0.30 to 0.45)
Land water storage anomaly due to reservoirs ( $LWSA_{res}$ )	-0.21	-0.10 (-0.11 to -0.10)	-0.02 (-0.03 to -0.02)
Land water storage anomaly due to water abstraction ( $LWSA_{abs}$ )	0.14 (0.12 to 0.17)	0.30 (0.25 to 0.35)	0.39 (0.33 to 0.46)

### 3.2.4 Relation between climate and land water storage

By comparing precipitation anomalies to  $LWSA_{clim}$ , we found a correlation of  $r = 0.63$  with GPCC precipitation (Fig. 7, blue curves) and  $r = 0.72$  with CRU precipitation (Fig. 7, pink curves). Furthermore, we found a correlation of  $r = 0.87$  by comparing the difference between the two precipitation anomaly time series to the difference between the two  $LWSA_{clim}$  time series. From these results, we deduce that precipitation is most likely the main driver of  $LWSA_{clim}$  at global scale.

**Deleted:** a

**Deleted:** 5

**Deleted:** Table 5: Linear trends of contribution of TWSA, LWSA,  $LWSA_{clim}$ ,  $LWSA_{hum}$ ,  $LWSA_{res}$ ,  $LWSA_{abs}$  and individual water storage compartments to OMC over three periods (1948–1975, 1976–2002 and 2003–2016). Positive trends translate to ocean mass gain, whereas negative trends translate to ocean mass loss. Ensemble ranges are given in parentheses. Estimates are given in millimetres of sea level equivalent per year ( $mm\ SLE\ yr^{-1}$ ).

**Moved (insertion) [4]**

**Deleted:** W

**Deleted:** between GPCC precipitation anomalies and  $LWSA_{clim}$  based on with

**Deleted:** ,

**Deleted:** of

**Deleted:** ture

**Deleted:** 8

**Deleted:** By comparing global precipitation anomalies from CRU TS3.10 and GPCC v5, Harris et al. (2014) identified a correlation of  $r = 0.88$  over 1951–2009 (see their Table II and Figure 10). We identified a correlation of  $r = 0.86$  over 1948–2016 between the precipitation time series used in this study. This is noteworthy, given the fact that GPCC is based on a much larger number of station records than CRU. Note that the high correlation between the two data sets means that our ensemble underestimates the uncertainty in global TWSA due to precipitation input data.

**Deleted:** Harris et al. (2014) identified a correlation of  $r = 0.88$  over 1951–2009 (see their Table II and Figure 10). We identified a correlation of  $r = 0.86$  over 1948–2016 between the precipitation time series used in this study. This is noteworthy, given the fact that GPCC is based on a much larger number of station records than CRU. Note that the high correlation between the two data sets means that our ensemble underestimates the uncertainty in global TWSA due to precipitation input data.

**Deleted:** (2014) identified a correlation of  $r = 0.88$  over 1951–2009 (see their Table II and Figure 10). We identified a correlation of  $r = 0.86$  over 1948–2016 between the precipitation time series used in this study. This is noteworthy, given the fact that GPCC is based on a much larger number of station records than CRU. Note that the high correlation between the two data sets means that our ensemble underestimates the uncertainty in global TWSA due to precipitation input data.

**Deleted:** (2014) identified a correlation of  $r = 0.88$  over 1951–2009 (see their Table II and Figure 10). We identified a correlation of  $r = 0.86$  over 1948–2016 between the precipitation time series used in this study. This is noteworthy, given the fact that GPCC is based on a much larger number of station records than CRU. Note that the high correlation between the two data sets means that our ensemble underestimates the uncertainty in global TWSA due to precipitation input data.

**Deleted:** identified a correlation of  $r = 0.88$  over 1951–2009 (see their Table II and Figure 10). We identified a correlation of  $r = 0.86$  over 1948–2016 between the precipitation time series used in this study. This is noteworthy, given the fact that GPCC is based on a much larger number of station records than CRU. Note that the high correlation between the two data sets means that our ensemble underestimates the uncertainty in global TWSA due to precipitation input data.

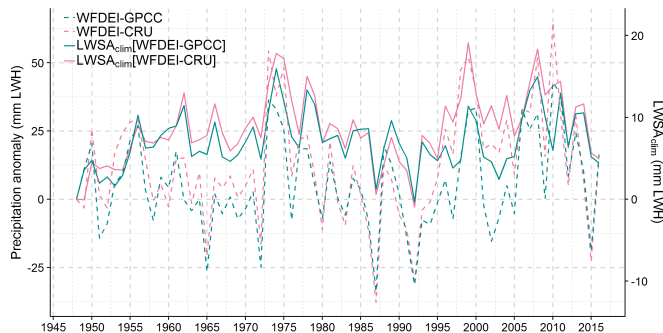


**Figure 7:** Correlation between global annual climate-driven LWSA and precipitation anomaly, 1948 to 2016. Precipitation (rainfall plus snowfall) anomalies correspond to the WFDEI-GPCC and WFDEI-CRU forcings used in this study (Section 2.1.1). Climate-driven LWSA ( $LWSA_{clim}[WFDEI-GPCC]$  and  $LWSA_{clim}[WFDEI-CRU]$ ) were obtained with integrated WaterGAP in naturalized mode (see Table 2). Anomalies are relative to the year 1948 and given in millimetres of land water height (mm LWH).

Furthermore, given that previous studies have shown that  $LWSA_{clim}$  is affected by internal multi-year climate variability such as ENSO (Cazenave and Llovel, 2010; Llovel et al., 2011; Cazenave et al., 2012; Boening et al., 2012), we also looked at the relation between the residual signal (i.e. non-linear interannual variability) in TWSA (Figure 8a) and short-term natural climate variability induced by ENSO and expressed as Multivariate ENSO Index (MEI) version 2 intensities (Wolter and Timlin, 1993; Wolter and Timlin, 1998) over 1980–2016 (Figure 8b). The period was chosen according to the availability of MEI data. Based on the latter, we identified four major La Niña events ( $MEI < 1$ ) and five major El Niño events ( $MEI > 1$ ) during 1980–2016. According to our results, part of the signature in simulated TWSA interannual variability reflects ENSO-driven climate variability. We can observe a continental water storage decrease during El Niño phases that most certainly reflects the rainfall deficit over the continents (mostly the tropics) observed during this type of event, as opposed to a continental water storage increase during La Niña phases, as a response to increased rainfall. Differences due to precipitation input data are significant (Figure 8a). The impact of the La Niña event of 1988/1989 is more prominent with GPCC precipitation; this is related to higher precipitation anomalies (i.e. wetter conditions) with GPCC (Figure 7). The opposite is observed during the La Niña event of 1998/2000, and can be explained in the same way. Note that there is no difference between the two irrigation variants, because  $LWSA_{hum}$  mainly affects long-term linear variability (Figures 5c and 6).

**Deleted:** ENSO (Llovel et al., 2011; Cazenave et al., 2012; Boening et al., 2012)...

**Moved (insertion) [5]**

**Deleted:** Previous studies have shown that  $LWSA_{clim}$  is affected by internal multi-year climate variability such as ENSO (Llovel et al., 2011; Cazenave et al., 2012; Boening et al., 2012). We looked at the relation between the residual signal (i.e. non-linear inter-annual variability) in TWSA (Figure 9a) and short-term natural climate variability related to ENSO and expressed as Multivariate ENSO Index (MEI) version 2 intensities (Wolter and Timlin, 1993; Wolter and Timlin, 1998) over 1980–2016 (Figure 9b). The period was chosen according to the availability of MEI data. The MEI, which combines both oceanic and atmospheric variables, is an indicator of ENSO intensity. Note that, during El Niño phases, TWS tends to decrease; this is due to a rainfall deficit over the continents (mostly the tropics). During La Niña phases, the opposite is observed. ...

**Deleted:** (Llovel et al., 2011; Cazenave et al., 2012; Boening et al., 2012). We looked at the relation between the residual signal (i.e. non-linear inter-annual variability) in TWSA (Figure 9a) and short-term natural climate variability related to ENSO and expressed as Multivariate ENSO Index (MEI) version 2 intensities (Wolter and Timlin, 1993; Wolter and Timlin, 1998) over 1980–2016 (Figure 9b). The period was chosen according to the availability of MEI data. The MEI, which combines both oceanic and atmospheric variables, is an indicator of ENSO intensity. Note that, during El Niño phases, TWS

**Deleted:** . We looked at the relation between the residual signal (i.e. non-linear inter-annual variability) in TWSA (Figure 9a) and

**Deleted:** (Wolter and Timlin, 1993; Wolter and Timlin, 1998) over 1980–2016 (Figure 9b). The period was chosen according to the

**Deleted:** over 1980–2016 (Figure 9b). The period was chosen according to the availability of MEI data. The MEI, which combines

**Deleted:** MEI intensities

**Deleted:** to

**Deleted:** -

**Deleted:** ,

**Deleted:** 8

**Deleted:** Moreover, n

**Deleted:** ures

**Deleted:** b

**Deleted:** By studying the GRACE record at regional scale, Wang et al. (2018) showed that the sensitivity to ENSO modulations is

**Deleted:** Wang et al. (2018) showed that the sensitivity to ENSO modulations is more prominent in the global exorheic (i.e. draining into the ocean)

**Deleted:** (2018) showed that the sensitivity to ENSO modulations is more prominent in the global exorheic (i.e. draining into the ocean)

**Deleted:** (2018) showed that the sensitivity to ENSO modulations is more prominent in the global exorheic (i.e. draining into the ocean)

**Deleted:** showed that the sensitivity to ENSO modulations is more prominent in the global exorheic (i.e. draining into the ocean)

**Deleted:** (Llovel et al., 2011).

**Deleted:** .

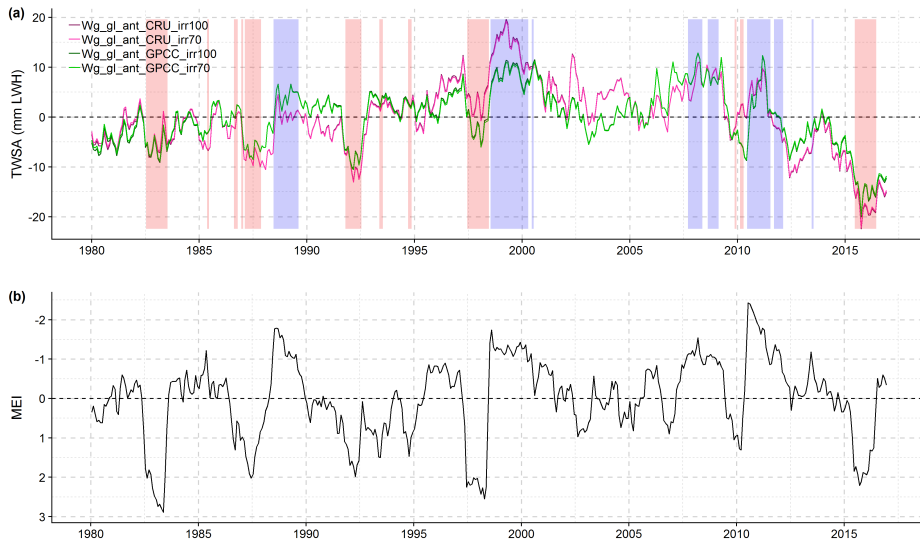


**Figure 8:** Relation between global monthly TWSA and ENSO, January 1980 to December 2016. (a) Residual TWSA (non-linear interannual variability) computed with four variants of integrated WaterGAP (Wg\_gl) in anthropogenic mode (Table 1). Anomalies are relative to the mean over January 1990 to December 2010 and given in millimetres of land water height (mm LWH). (b) Intensities in Multivariate ENSO Index (MEI) version 2 (produced by NOAA). Positive MEI values indicate El Niño and negative values indicate La Niña phases. El Niño (red) and La Niña (blue) phases are highlighted in plot (a) whenever the MEI gets larger than 1 or smaller than -1, respectively. Note the reversed vertical axis in (b).

### 3.2.5 Contributions of individual water storage compartments

Among the nine water storage compartments in Wg\_gl, largest absolute change over the period 1948–2016 is mass loss from glaciers, i.e. a positive contribution of LGWSA to ocean mass change equivalent to 30 mm SLE (Figure 9a). The second largest is groundwater depletion, with a decrease of 13–19 mm SLE depending on the irrigation assumption. The third largest (with opposite sign) is water impoundment in reservoirs, which added 8 mm SLE to the continents. In the storages of surface water bodies, there are only very small differences due to the irrigation variant. Apart from LGWSA, GWSA and ReWSA, the rest of the contributions are marginal, with negative contributions from the river and wetland storages, and positive contributions from the soil, lake and snow storages (Figure 9b). Differences related to precipitation forcing, which are more visible in Figure 9b, exist in all storages except for the glacier one, which is not affected by the different WaterGAP precipitation forcings as it is a direct input to WaterGAP.

Moved (insertion) [6]

Deleted: -

Deleted: to TWSA

Deleted: decrease

Deleted: by

Deleted: 7

Deleted: SWB

Deleted: water storage compartments have only a marginal

Deleted: 7

Deleted: 7

Deleted: storage

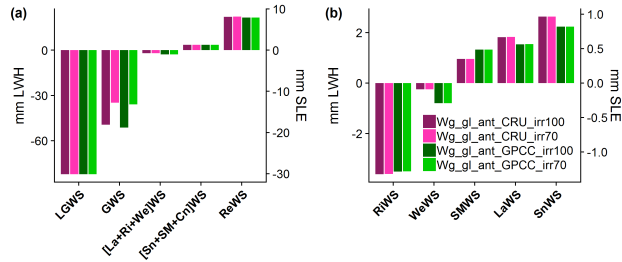


**Figure 9:** Global cumulated water storage change in individual water storage compartments, 1948 to 2016. Estimates were obtained with four variants of integrated WaterGAP in anthropogenic mode (Table 1). (a) Water storage (WS) change in glacier (LG), groundwater (G), aggregate of lake (La), river (Ri) and wetland (We), aggregate of snow (Sn), soil moisture (SM) and canopy (Cn), and reservoir (Re) compartments. (b) Water storage change in river, wetland, soil moisture, lake and snow storages. Canopy storage is not included because the cumulated change is in the order of  $1 \cdot 10^{-3}$  mm LWH. Estimates are given in millimetres of land water height (mm LWH) and of sea level equivalent (mm SLE).

#### 4. Discussion

##### 4.1 TWSA temporal components

###### 4.1.1 Linear trend: comparison to independent estimates

If we consider the linear trend of the ensemble mean,  $Wg\_gl$  overestimates the positive contribution of TWSA to ocean mass change by 30–50% as compared to the GRACE TWSA trends from this study (Tables 3 and 5). However, if we assume 70% deficit irrigation in groundwater depletion regions and GPCC precipitation, the simulated trend is within the GRACE uncertainty bounds (Table 3). We consider this variant more likely because 1) GPCC is based on a much larger number of station records than CRU (see Figure 2 of Schneider et al., 2014) and 2) it seems implausible that farmers in groundwater depletion areas have optimal irrigation conditions (Döll et al., 2014). Despite this, we included this assumption in the design of the model variants as an upper-bound of groundwater depletion (Figure 9). GRACE estimates from other studies (Rietbroek et al., 2016; Reager et al., 2016; Blazquez et al., 2018) suggest much smaller continental water mass losses to oceans (Table 5). Differences between GRACE-based TWSA trends from this study and from independent sources are of the same order of magnitude as differences between GRACE- and model-based TWSA trends from this study. This suggests that GRACE-based TWSA trends are very sensitive to the multiple processing parameters applied to the GRACE Level-2 data (Blazquez et al., 2018).

The overestimation of the TWSA positive contribution by  $Wg\_gl$  may arise from uncertainty in both the LWSA and LGWSA components. There is a rather good agreement between LGWSA trends from GGM, on the one hand, and from Dieng et al. (2017) and Reager et al. (2016), on the other hand. The agreement to Dieng et al. (2017) is not surprising, since

Deleted: : seasonality and long-term variability

Deleted: In terms of

Deleted: OMC

Deleted: 6

Deleted: GWD

Deleted: assuming

Deleted: GWD

Deleted: seems implausible

Deleted: GWD

Deleted: 7

Deleted: 6

Deleted: than

430 their estimates were obtained by averaging three data sets, including a GGM data set used by Marzeion et al. (2015) (update  
 435 from Marzeion et al., 2012). Nevertheless, according to the GRACE-based estimates from Rietbroek et al. (2016) and  
 Schrama et al. (2014), GGM overestimates the LGWSA contribution. The more recent non-GRACE-based estimates from  
 Bamber et al. (2018) and Zemp et al. (2019) are in better agreement with the estimates from GGM, even though still too  
 small in comparison (Table 5).

435 **Table 5:** Comparison between trends of TWSA, LGWSA, LWSA, LWSA<sub>hum</sub> and LWSA<sub>clim</sub> from the literature and this study (in  
 parentheses). TWSA trends from this study were derived from GRACE observations and integrated WaterGAP (Wg\_gl) in anthropogenic  
 mode. LWSA trends were obtained by subtracting LGWSA trends from TWSA trends based on either GRACE or Wg\_gl. LWSA<sub>clim</sub>  
 trends were obtained by subtracting LWSA<sub>hum</sub> based on Wg\_gl from LWSA based on either GRACE or Wg\_gl. Positive trends translate to  
 5440 ocean mass gain, whereas negative trends translate to ocean mass loss. Estimates are given in millimetres of sea level equivalent per year  
 (mm SLE yr<sup>-1</sup>).

Deleted: 6  
 Deleted: this study and  
 Deleted: from  
 Deleted: from

Study	Method	Time period	TWSA	LGWSA	LWSA	LWSA <sub>hum</sub>	LWSA <sub>clim</sub>
Dieng et al. (2017)	I + M	Jan 1993– Dec 2015	1.00 (0.91 <sup>c</sup> )	0.76 ± 0.08 (0.62 ± 0.03 <sup>c</sup> )	0.24 ± 0.09 (0.29 <sup>c</sup> )		0.12 (-0.05 <sup>c</sup> )
		Jan 2004– Dec 2015	1.03 (0.81 ± 0.20 <sup>b</sup> /1.19 <sup>c</sup> )	0.78 ± 0.07 (0.76 ± 0.03 <sup>c</sup> )	0.25 ± 0.08 (0.05 <sup>b,c</sup> /0.43 <sup>c</sup> )		
Rietbroek et al. (2016)	G	Apr 2002– Jun 2014 <sup>a</sup>	0.09 (0.64 ± 0.20 <sup>b</sup> /0.94 <sup>c</sup> )	0.38 ± 0.07 (0.74 ± 0.03 <sup>c</sup> )	-0.29 ± 0.26 (-0.10 <sup>b,c</sup> /0.20 <sup>c</sup> )		
Reager et al. (2016)	G + I	Apr 2002– Nov 2014 <sup>a</sup>	0.32 ± 0.13 (0.64 ± 0.20 <sup>b</sup> /0.97 <sup>c</sup> )	0.65 ± 0.09 (0.74 ± 0.03 <sup>c</sup> )	-0.33 ± 0.16 (-0.10 <sup>b,c</sup> /0.23 <sup>c</sup> )		-0.71 ± 0.20 (-0.41 <sup>b,c</sup> /-0.09 <sup>c</sup> )
Blazquez et al. (2018)	G	Aug 2002– Jun 2014 <sup>a</sup>	0.07 ± 0.12 <sup>d</sup> (0.61 ± 0.20 <sup>b</sup> /0.93 <sup>c</sup> )				
Schrama et al. (2014)	G	Jan 2003– Dec 2013		0.44 ± 0.03 (0.75 ± 0.03 <sup>c</sup> )			
Bamber et al. (2018)	I	Sep 2002– Aug 2006 <sup>a</sup>		0.48 ± 0.09 (0.71 ± 0.03 <sup>c</sup> )			
		Sep 2007– Aug 2011		0.55 ± 0.08 (0.73 ± 0.03 <sup>c</sup> )			
Zemp et al. (2019)	O	Sep 2006– Aug 2016		0.56 ± 0.04 (0.80 ± 0.03 <sup>c</sup> )			
Dieng et al. (2015)	B	Jan 2003– Dec 2013			0.30 ± 0.18 (-0.11 <sup>b,c</sup> /0.18 <sup>c</sup> )		
Wada et al. (2016)	I	Jan 1993– Dec 2010				0.12 ± 0.04 (0.31 <sup>c</sup> )	
IPCC AR5	I	Jan 1993– Dec 2011				0.38 ± 0.12 (0.31 <sup>c</sup> )	

<sup>a</sup> Only three (CSR\_r106sh, ITSG\_2018 and JPL\_r106sh) out of four GRACE solutions were considered (GFZ\_r106sh was excluded because of lack of values in 2002). <sup>b</sup> Trends based on GRACE data sets used in this study. <sup>c</sup> Trends based on modelled data sets (Wg\_gl) used in this study. <sup>d</sup> Uncertainty estimates in the source paper are expressed in 1.65σ. Here, they are expressed in 1σ. I: multiple independent estimates; M: modelling; G: GRACE data; O: observations; B: global water mass budget.



5450 The discrepancy between GRACE- and model-based TWSA trends from this study is also reflected in the LWSA trends. If LGWSA is subtracted from TWSA of  $Wg_{gl}$ , a mass loss on land is computed, while a (small) mass gain on land results if GRACE-based TWSA is used instead (Table S). This can be related to the findings of Scanlon et al. (2018), which show that LWSA trends summed over 183 basins worldwide (~63% of global continental area excluding the ice sheets) indicate a mass gain on land for GRACE but a mass loss on land for models. The LWSA trends from Rietbroek et al. (2016) and Reager et al. (2016) suggest a higher water mass gain on continents than our GRACE-based trends, reflecting the discrepancy in TWSA trends, which is not compensated by smaller glacier mass losses in these two studies. On the other hand, it is noteworthy that our model-based LWSA trends are in good agreement with other non-GRACE-based trends, namely the ones from Dieng et al. (2015) and Dieng et al. (2017) (Table S).

5460 The presumed overestimation of the LWSA positive contribution to ocean mass change by  $Wg_{gl}$  may reflect an overestimation of the  $LWSA_{hum}$  positive contribution and/or an underestimation of the  $LWSA_{clim}$  negative contribution. Our  $LWSA_{hum}$  trend is in good agreement with the one reported by the IPCC AR5, but overestimated according to the trend of Wada et al. (2016) (Table S). Wada et al. (2016) argued that the  $LWSA_{hum}$  positive contribution of the IPCC AR5 is probably overestimated by a factor of 3, and that this is partly due to the fact that the IPCC AR5 assumes that 100% of groundwater depletion ends up in the ocean, whereas their study shows that only 80% of it actually does. We estimate a groundwater depletion trend of 0.39 mm SLE  $yr^{-1}$  over 2003–2016 (see Table S3 in the supplementary information), which is within the uncertainty bounds of the trend reported by Wada et al. (2016),  $0.30 \pm 0.10$  mm SLE  $yr^{-1}$  over 2002–2014, even if slightly higher. Concerning the  $LWSA_{clim}$  component, Dieng et al. (2017) computed a positive contribution, whereas  $Wg_{gl}$  computed a negative contribution, suggesting differences between models. Moreover, the trend from Reager et al. (2016) suggests that  $Wg_{gl}$  underestimates continental water mass gain due to climate variability; by assuming GRACE-based TWSA, we obtain a more negative  $LWSA_{clim}$  trend, however still differing from the estimate of Reager et al. (2016) by roughly a factor of 2 (Table S).

#### 4.1.2 Seasonality and interannual variability

5475 The small discrepancy between GRACE and  $Wg_{gl}$  in terms of TWSA seasonality (Figure 4b) is partly due to differences in seasonal amplitude. For instance, some years (2006, 2009 and 2011) show smaller simulated seasonal amplitude than what is observed by GRACE. Although we did not investigate this matter at regional scale, we speculate that this might be due to a systematic underestimation of seasonal amplitude in tropical basins by WaterGAP, where the seasonal signal is strongest, resulting from insufficient storage capacity (Scanlon et al., 2019). At global scale, however, underestimation in tropical basins might be compensated by overestimation in other types of basin.

5480 The most prominent discrepancies between global mean monthly TWSA from GRACE and  $Wg_{gl}$  are observed in the residual signal, which contains the interannual variability (Figure 4f). The interannual variability comes almost completely from the LWSA component (Figures 4e-f), and more specifically from its climate-driven component ( $LWSA_{clim}$  in Fig. 5c) at

**Deleted:** The overestimation of the TWSA positive contribution by  $Wg_{gl}$  may arise from uncertainty in both the LWSA and LGWSA components. There is a rather good agreement between the LGWSA trend from GGM, on the one hand, and from Dieng et al. (2017) and Reager et al. (2016), on the other hand. The agreement to Dieng et al. (2017) is not surprising, since their estimates were obtained by averaging three data sets, including a GGM data set used in Marzeion et al. (2015) (update from Marzeion et al., 2012). Nevertheless, according to the GRACE-based estimates from Rietbroek et al. (2016) and Schrama et al. (2014), GGM overestimates the LGWSA contribution. The more recent non-GRACE-based estimates from Bamber et al. (2018) and Zemp et al. (2019) are in better agreement with the estimates from GGM, even though still too small in comparison (Table 6).

**Deleted:** 6

**Deleted:** are positive

**Deleted:** (

**Deleted:** )

**Deleted:** negative (

**Deleted:** )

**Deleted:** (Table 6)

**Deleted:** (Table 6)

**Deleted:** 6

**Deleted:** OMC

**Deleted:** 6

**Deleted:** GWD

**Deleted:** GWD ends up in the ocean

**Deleted:** GWD

**Deleted:** 5

**Deleted:** closer to

**Deleted:** 6

**Deleted:** <#>Residual: long-term non-linear variability

**Deleted:** (Figure 4f)

**Deleted:** -

**Deleted:** -

**Deleted:** and 4

**Deleted:** ure

**Deleted:** b

520 global scale. Cazenave (2018) pointed out that this is arguably the most difficult component in the land water budget to  
quantify. Humphrey et al. (2016) show that interannual anomalies in the GRACE signal can be correlated to anomalies in  
precipitation (positive correlation) and near-surface temperature (negative correlation); our results confirm the positive  
correlation to precipitation (Fig. 7). The discrepancy between the residual signal in GRACE and Wg\_gl is more prominent in  
some years (Figure 4f). This may reflect the occurrence of ENSO events; in particular, we can identify the intense La Niña  
event of 2010/2011 and the intense El Niño event of 2015/2016. If we rely on the validity of the GRACE time series, despite  
530 the significant gaps in the data for both events, then it can be inferred that, even though Wg\_gl reproduces the events to some  
extent, it underestimates their intensity. By studying the GRACE record at regional scale, Wang et al. (2018) showed that the  
sensitivity to ENSO modulations is more prominent in the global exorheic (i.e. draining into the ocean) system, as opposed  
to the global endorheic (i.e. landlocked) system (see their Figure 2). Within the exorheic system, tropical basins (particularly  
the Amazon) are more sensitive to these modulations (Llovel et al., 2011). This suggests the difficulty of correctly simulating  
not only seasonal (Scanlon et al., 2019), but only annual amplitudes in tropical basins by WaterGAP.

#### 4.2 Limitations of study

535 Simulated global TWSA is the result of aggregating water storage change estimates corresponding to nine individual water  
storage compartments and 64432 grid cells. There is uncertainty in each single estimate (due to uncertain climate input,  
assumptions related to water use, model parameters etc.). However, errors in individual storage compartments and at smaller  
spatial scales may average out once aggregated at global scale. In this section, we discuss the limitations of our  
reconstruction of global TWSA time series and thus mass transfer from continents to oceans. Limitations in our approach are  
related to the integration of glacier data as an input to WaterGAP, to the global models (GGM and WaterGAP) used to  
compute LGWSA and LWSA and to missing components that were not accounted for in this study.

##### 4.2.1 Glacier data integration approach

540 The glacier data integration significantly improved the simulation of the global mean TWSA linear trend by WaterGAP  
(Figure 4c-d). However, this approach does not give appreciably different results from simply adding the separately  
estimated LGWSA and LWSA components (hereafter the “addition approach”) at global scale (Figure 3). According to the  
data used in this study, we estimate that glaciers cover 0.38% of the global continental area (excluding the ice sheets), which  
is smaller than the estimate of Bamber et al. (2018), amounting to 0.50%. However, the area effectively accounted for by  
545 integrated WaterGAP amounts to 0.34% (~11% of global glacier area is neglected, see Section 2.3.1), resulting in a  
reduction of its global land area ranging from 0.39% in 1948 to 0.34% in 2016. Thus, it is not strange that the reduction of  
the land area had an insignificant effect at global scale. We speculate that, at basin scale, the glacier data integration  
approach might show significantly different results from the addition approach.

550 Moreover, our approach has limitations regarding the fate of the internally calculated glacier runoff. One of the sources of  
uncertainty related to the contribution of glaciers to sea-level rise is the interception of glacier runoff by land; it is still vastly

Deleted: -

Deleted: we discuss the relation between precipitation anomalies and inter-annual variability in Section 6.3.1...

Deleted: Furthermore, inter-annual fluctuations in LWS can reflect the occurrence of atmospheric circulation patterns, like the El Niño Southern Oscillation (Cazenave and Llovel, 2010; Llovel et al., 2011; Cazenave et al., 2012). ...

Deleted: I

Deleted: (positive peak indicating a water mass gain on land)

Deleted: (negative peak indicating a water mass loss on land)

Deleted: (Scanlon 2019)

Deleted: We discuss further the relation between the El Niño Southern Oscillation (ENSO) occurrence and inter-annual variability in Section 6.3.2....

Deleted:

Deleted: about

Deleted: time series of

Deleted: and 4

Deleted: 3.3

Deleted: SLR

assumed that glacier runoff flows directly to the ocean, with no delay or interception by water storage compartments (Church et al., 2013). In our approach, we assume that glacier runoff is intercepted by surface storages, but not by sub-surface (soil and groundwater) storages. We made this assumption because we have no means of assessing how much glacier runoff is intercepted by sub-surface storages at global scale.

#### 5575 4.2.2 Global modelling of LGWSA

Previous studies (Marzeion et al., 2015; Slangen et al., 2017) have shown agreement between GGM and other global glacier models. For instance, according to Marzeion et al. (2015), the reconstruction of global glacier mass change during the twentieth century by GGM is consistent with the ones obtained from other methods of reconstruction (see their Figure 1). However, note that this might simply mean that the methods are consistently wrong. In addition, using an extrapolation of glaciological and geodetic observations, Zemp et al. (2019) estimate that glaciers (outside the ice sheets) contributed  $23 \pm 14$  mm SLE to global-mean sea-level rise, from 1961 to 2016. We estimate a contribution of 25 mm SLE with GGM over the same period, which is remarkably consistent with the estimate from Zemp et al. (2019). Furthermore, our evaluation of GGM performance (Section 3.1.1) shows that this model can reproduce well the observed mean seasonality of winter accumulation and summer ablation; this is not always the case for global glacier models (Fig.4, Hirabayashi et al., 2010).

5585 Despite the fact that we consider GGM estimates to be state-of-the-art, they are subject to multiple sources of uncertainty. Input data (climate forcing and glacier outlines), simplification of physics in the model, observation data used for calibration and the calibration itself are among the main sources. GGM includes uncertainty estimates related to annual glacier mass change time series. However, we did not include these uncertainty estimates in our assessment (we only included the trend uncertainty, which corresponds to a  $1\sigma$  standard uncertainty) for consistency reasons (i.e. most data sets used for the assessment have unknown uncertainties).

#### 5590 4.2.3 Global modelling of LWSA

Uncertainty in WaterGAP estimates is related to both the  $LWSA_{hum}$  and  $LWSA_{clim}$  components. Modelling of groundwater depletion, which is both related to climate variability and human water use, is of key importance, as global water storage trends computed with WaterGAP are particularly sensitive to these variations (Müller Schmied et al., 2014). Global groundwater depletion is highly linked to irrigation groundwater abstraction. The estimation of gross and net irrigation groundwater abstraction is not a trivial task, as it relies mainly on statistical data and assumptions, and depends on climate input (Döll et al., 2016). Siebert et al. (2010) estimated that 43% of the total consumptive irrigation water use comes from groundwater. The rate of global groundwater depletion has been subject to much debate (Döll et al., 2014; Wada et al., 2017). According to Wada et al. (2017), most studies likely overestimated the cumulative contribution of groundwater depletion to global sea-level rise during the twentieth and early twenty-first century. Our groundwater depletion estimates are very likely overestimated under optimal irrigation, however more robust under 70% deficit irrigation (Döll et al., 2014). Our estimate of  $0.32 \text{ mm SLE yr}^{-1}$  over 2003–2016 under 70% deficit irrigation (see Table S3 in the supplementary

Deleted: SLR

Deleted: 4.1

Deleted: GWD

Deleted: GWD

Deleted: In the past, t

Deleted: and regional

Deleted: GWD

Deleted: GWD

Deleted: SLR

Deleted: GWD

information) is in good agreement with the study of van Dijk et al. (2014), who estimated a trend of 0.26 mm SLE yr<sup>-1</sup> over 2003–2012 using a data assimilation framework to integrate water balance estimates from GRACE and several GHMs.

5615 Modelling reservoir storage and operation is also subject to multiple sources of uncertainty (e.g. quality of reservoir data  
base, algorithms and assumptions used in model). In the present study, we did not include model variants differing from one  
another in the way reservoirs are handled. Wada et al. (2017) estimated a global reservoir storage capacity of 7968 km<sup>3</sup> (~22  
mm SLE) until 2014. WaterGAP has a global reservoir storage capacity of 5764 km<sup>3</sup> (~16 mm SLE), as it only simulates the  
largest 1082 man-made reservoirs (Section 2.1.1). Furthermore, by assuming that on average 85% of the reservoir capacity is  
5620 used and taking into account seepage (i.e. adding additional water that seeps underground), Wada et al. (2017) estimated a  
potential total water impoundment in reservoirs of ~29 mm SLE. Upon application of the reservoir operation algorithm  
implemented in WaterGAP, we estimate an actual total water impoundment of ~10 mm SLE, which corresponds to roughly  
63% of the global reservoir capacity. Wada et al. (2017) might overestimate the additional water due to seepage, as well as  
the fraction of the design capacity that is in reality filled (85% according to their assumption). However, the estimate of our  
5625 study is likely an underestimation of the impoundment of water in man-made reservoirs because WaterGAP only simulates  
the largest reservoirs and does not account for seepage. In addition, WaterGAP incorporates the reservoirs from the GRanD  
v1.1 database, but not the additional ones from the new GRanD v1.3 release (<http://globaldamwatch.org>). GRanD v1.3  
includes 458 additional reservoirs as compared to GRanD v1.1. Out of 458 reservoirs, 447 were put in operation between  
1948 and 2016. Out of these 447 reservoirs, 173 have a total capacity of at least 0.5 km<sup>3</sup> and thus would be simulated as  
5630 reservoirs by WaterGAP. The cumulated total capacity of these 173 reservoirs amounts to 599 km<sup>3</sup>. The remaining 274  
smaller reservoirs have a cumulated total capacity of 62 km<sup>3</sup>. Out of the 173 large reservoirs, 164 were put in operation  
between 2000 and 2016. Taking into account that we computed an actual total water impoundment of roughly 63% of the  
global reservoir capacity, we can infer that incorporating the additional large reservoirs would lead to an additional  
impoundment of 378 km<sup>3</sup> (1.05 mm SLE) over 1948–2016, thus increasing total impoundment of water from 8 to 9 mm SLE,  
5635 i.e. from 22 mm LWH to 25 mm LWH (compare Fig. 6). Most of the additional impoundment not taken into account in this  
study (369 km<sup>3</sup>, 1.02 mm SLE) occurred in the period 2000–2016. Therefore, WaterGAP is expected to overestimate the  
positive contribution of water storage on continents during the GRACE period by approximately 0.06 mm SLE/yr, which  
explains part of the overestimation as compared to GRACE (Table 3).

LWSA<sub>clim</sub> is largely affected by uncertain climate input data. As stated by Döll et al. (2016), this remains one of the main  
5640 challenges in the development and application of GHMs. Precipitation and radiation data have been identified as strong  
drivers of water storage change (Müller Schmied et al., 2014; Müller Schmied et al., 2016; Humphrey et al., 2016). Our  
assessment accounts for part of the uncertainty related to precipitation input data by considering two different climate  
forcings (WFDEI-GPCC and WFDEI-CRU). By comparing global precipitation anomalies from CRU TS3.10 and GPCC v5,  
Harris et al. (2014) identified a correlation of  $r = 0.88$  over 1951–2009 (see their Table II and Figure 10). We identified a  
5645 correlation of  $r = 0.86$  over 1948–2016 between the precipitation time series used in this study. Note that the high correlation

**Deleted:** Our estimate of total water impoundment might be underestimated because WaterGAP only simulates the largest reservoirs and because it does not account for seepage. On the other hand, ...

between the two data sets means that our ensemble underestimates the uncertainty in global TWSA due to precipitation input data. However, in general we believe that WFDEI-GPCC is likely to be more reliable than WFDEI-CRU because 1) the monthly time series of gridded precipitation from GPCC used to bias-adjust WFDEI-GPCC are based on more observation stations (Müller Schmied et al., 2016) and 2) GRACE-derived trends of TWSA in 186 large river basins correlate much more with trends computed by WaterGAP if GPCC precipitation is used (Scanlon et al., 2018). Despite this, both forcings are not well suited for trend analysis as a consequence of the bias correction, which significantly affects trends of climatic variables such as temperature and precipitation (Hempel et al., 2013; Weedon et al., 2014). TWSA trends simulated by WaterGAP are most likely affected by this caveat regarding the climate forcing. Moreover, note that, given the complex interactions and feedbacks in the climate system, we could not, unlike for LWSA<sub>hum</sub>, isolate the different components of

LWSA<sub>clim</sub>.

#### 4.2.4 Missing components

The Caspian Sea (largest endorheic lake worldwide), which was one of the largest contributors to global lake water storage loss during the twentieth century (Milly et al., 2010), is missing from our assessment because the WaterGAP model grid, based on the WATCH-CRU land-sea mask, does not include it. Its contribution to sea-level rise, if a complete loss to oceans via vapour transfer is assumed, was previously estimated to be 0.06 mm SLE yr<sup>-1</sup> over 1992–2002 (Milly et al., 2010) and 0.071 ± 0.006 mm SLE yr<sup>-1</sup> over April 2002–March 2016 (Wang et al., 2018), including only surface water variations, and 0.109 ± 0.004 mm SLE yr<sup>-1</sup> over 2002–2014 (Wada et al., 2017), including variations in both surface water and the influenced groundwater. The GRACE-based solutions used in this study do consider the Caspian Sea as a lake and include its mass changes. Our net-loss estimates from lake surface integration amount to 0.055 ± 0.003 mm SLE yr<sup>-1</sup> (fit uncertainty) over 2003–2016 on average over all four solutions (see Figures S3 and S4 in supplementary information), plus an unassessed leakage contribution (~20%). Note that, during the GRACE period, the underestimation of modelled mass loss on continents due to the missing Caspian Sea is almost compensated (in terms of linear trend) by the underestimation of modelled mass gain due to the missing reservoirs from GRanD v1.3 (Section 4.2.3).

Moreover, WaterGAP does not account for land cover change. This means that the impact of human-induced phenomena such as deforestation is neglected. Wada et al. (2017) estimated that net global deforestation contributed ~0.035 mm SLE yr<sup>-1</sup> to sea-level rise over 2002–2014 through runoff increase and water release from oxidation and plant storage. Using a dynamic global vegetation and water balance model, Rost et al. (2008) estimated that human-induced land cover change (mainly deforestation) reduced evapotranspiration by 2.8% and increased streamflow by 5.0% globally over 1971–2000.

#### 5. Conclusions

In order to quantify water transfers between continents and oceans over 1948–2016, we used a non-standard version of WaterGAP that is able to simulate the variations in all continental water storage compartments. The model was run under different assumptions of irrigation water use and with different precipitation input data sets to account for major hydrological

**Deleted:** wW ... [29]

**Deleted:** Nevertheless, we discuss about some of its main drivers in Section 6.3....

**Deleted:** TheIts contribution of this endorheic lake ...o sea-level rise, if a ... [30]

**Deleted:** (including variations in both surface water and the ... [31]

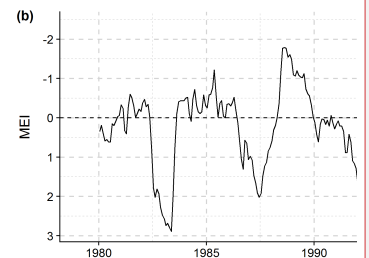
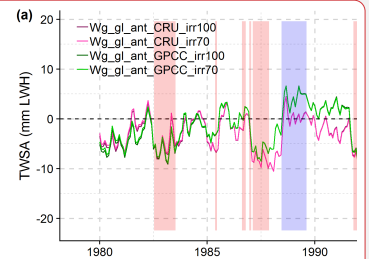
**Deleted:** anthropogenic

**Deleted:** , through runoff increase and water release from oxidat... [32]

**Moved up [4]:** We found a correlation of  $r = 0.63$  between GPCC anomalies and LWSA<sub>clim</sub> based on GPCC precipitation, and of  $r = 0.72$  with CRU precipitation (Figure 8). Furthermore, we found a correlation of  $r = 0.87$  by comparing the difference between the two

**Deleted:** Harris et al. (2014) identified a correlation of  $r = 0.88$  over 1951–2009 (see their Table II and Figure 10). We identified a correlation of  $r = 0.86$  over 1948–2016 between the precipitation time series used in this study. This is noteworthy, given the fact that ... [33]

**Moved up [5]:** Previous studies have shown that LWSA<sub>clim</sub> is affected by internal multi-year climate variability such as ENSO (Llovel et al., 2011; Cazenave et al., 2012; Boening et al., 2012). We looked at the relation between the residual signal (i.e. non-linear



**Deleted:**

**Moved up [6]:** Figure 9: Relation between global monthly TWSA and ENSO, January 1980 to December 2016. (a) Residual TWSA (non-linear inter-annual variability) computed with four variants of integrated WaterGAP (Wg\_gl) in anthropogenic mode (Table 1).

**Deleted:** the period 1948– to ...016, we integrated the output of ... [34]

025 modelling uncertainties. Time series of global mean monthly TWSA simulated with this ensemble were evaluated by  
comparing them to estimates from an ensemble of GRACE solutions over January 2003 to August 2016. A remarkable  
agreement between observed and modelled global mean monthly TWSA time series was found, with a high agreement with  
respect to seasonality and a likely small overestimation of the water storage decline for which a clear identification of the  
specific causes remains difficult, due to the complex feedbacks in the modelling system. On the other hand, Gutknecht et al.  
(2020) have demonstrated that replacing standard degree-1 coefficients with individual solutions during GRACE data  
processing can result in trends up to 0.3 mm SLE yr<sup>-1</sup> stronger than shown here.

Deleted: for the time period

Deleted: .

Deleted: We found no significant differences for global mean TWSA between our integrated modelling approach and simply adding the independently obtained LGWSA and LWSA components.

030 According to our model-based reconstruction, we conclude that continental water mass loss resulted in an ocean mass gain  
equivalent to 34–41 mm SLE during 1948–2016. Continents (including glaciers) lost water at an accelerated rate over time,  
with a contribution to ocean mass change of 0.18 mm SLE yr<sup>-1</sup> over 1948–1975, 0.58 mm SLE yr<sup>-1</sup> over 1976–2002 and 1.18  
mm SLE yr<sup>-1</sup> over 2003–2016 (Table 4). Global glacier mass loss accounted for 81% of the cumulated mass loss over 1948–  
035 2016, while the remaining 19% was lost from other continental water storage compartments (LWSA). LWSA over 1948–  
2016 were dominated by the impact of direct human interventions, namely water abstractions and impoundment of water in  
reservoirs. Continental mass loss due to water abstractions (15–21 mm SLE), mainly driven by irrigation water demand,  
showed an acceleration over time, with water lost mainly from groundwater (13–19 mm SLE). This mass loss offset  
continental mass gain from reservoir water impoundment (> 8 mm SLE), which showed a deceleration over time. Climate-  
040 driven LWSA is highly correlated to precipitation anomalies and is also influenced by multi-year modulations related to  
ENSO.

Deleted: OMC

Deleted: 5

Deleted: Changes in

Deleted: LWS

Deleted: from

Deleted: which

Deleted: LWS

Deleted: GWD (13–19 mm SLE) is strongly linked to water abstractions for irrigation purposes. ...

Deleted: variability in

Deleted: variations

Deleted: changes

Deleted: GWD

Deleted: changes

Deleted: interesting

045 Significant uncertainty in our assessment arises from the simulation of human-driven LWSA. Modelling of groundwater  
depletion, which is highly sensitive to irrigation water use assumptions, and of reservoir storage and operation is particularly  
challenging. Furthermore, simulated climate-driven LWSA are affected by uncertainty in the climate input data. Despite the  
limitations of our model-based approach and the remaining challenges, our assessment gives valuable insights on the main  
individual mass components and drivers of global water transfers from continents to oceans, as well as on possible routes for  
model improvement. More research is required to better constrain the simulation of human water use in GHMs. Finally,  
future research should go beyond the global scale by identifying the main regions contributing to water transfers between  
continents and oceans.

7050

#### Data availability

All GRACE-based and model-based data sets used in this study are available upon request from the corresponding author.

The glacier surface mass balance observational data used in this study are publicly available and can be downloaded from  
the following link, [https://wgms.ch/products\\_ref/glaciers/](https://wgms.ch/products_ref/glaciers/) (accessed on April 18<sup>th</sup> 2018). The MEI data used in this study are

Deleted: SMB

Deleted: ;

publicly available and can be downloaded from the following link: <https://www.esrl.noaa.gov/psd/enso/mei/data/meiv2.data> (accessed on July 10<sup>th</sup> 2019).

Deleted :

#### Author contribution

7080 PD and DC designed the study. DC conducted background research, implemented computer code for the integrated  
WaterGAP model version, conducted model simulations, prepared the WaterGAP data, performed the formal analysis and  
drafted the initial manuscript with substantial revisions from PD. BG, BM, HMS and PD discussed the results and edited the  
initial manuscript. BG prepared the GRACE data, provided a script for the computation of linear trends and the temporal  
7085 disaggregation of TWSA time series and contributed to the analysis of GRACE-based TWSA. PD contributed to the analysis  
of model-based TWSA and individual components. BM provided GGM simulation data and contributed to the analysis of  
glacier mass changes. HMS supported the implementation of computer code and provided a script for the aggregation of  
model-based TWSA over the global continental area. JM prepared the gridded glacier-related data.

#### Competing interests

The authors declare that they have no conflict of interest.

#### 7090 Acknowledgements

We thank Tim Trautmann from the Institute of Physical Geography of the Goethe University Frankfurt for his valuable  
comments to improve the first draft of the paper. We thank the investigators of the World Glacier Monitoring Service  
network as well as the NOAA Earth System Research Laboratory's Physical Sciences Division for free and open access to  
their data sets. This study was enabled by support from the European Space Agency (ESA) through its Sea-Level Budget  
7095 Closure CCI project (4000119910/17/I-NB).

#### References

- Bahr, D. B., Meier, M. F., and Peckham, S. D.: The physical basis of glacier volume-area scaling, 1997.
- Bamber, J. L., Westaway, R. M., Marzeion, B., and Wouters, B.: The land ice contribution to sea level during the satellite  
era, *Environ. Res. Lett.*, 13, 63008, doi:10.1088/1748-9326/aac2f0, 2018.
- 7100 Bergmann-Wolf, I., Zhang, L., and Dobslaw, H.: Global Eustatic Sea-Level Variations for the Approximation of Geocenter  
Motion from Grace, *Journal of Geodetic Science*, 4, doi:10.2478/jogs-2014-0006, 2014.
- Blazquez, A., Meyssignac, B., Lemoine, J. M., Berthier, E., Ribes, A., and Cazenave, A.: Exploring the uncertainty in  
GRACE estimates of the mass redistributions at the Earth surface: implications for the global water and sea level  
budgets, *Geophysical Journal International*, 215, 415–430, doi:10.1093/gji/ggy293, 2018.
- 7105 Boening, C., Willis, J. K., Landerer, F. W., Nerem, R. S., and Fasullo, J.: The 2011 La Niña: So strong, the oceans fell,  
*Geophys. Res. Lett.*, 39, n/a-n/a, doi:10.1029/2012GL053055, 2012.

- Caron, L., Ivins, E. R., Larour, E., Adhikari, S., Nilsson, J., and Blewitt, G.: GIA Model Statistics for GRACE Hydrology, Cryosphere, and Ocean Science, *Geophys. Res. Lett.*, 45, 2203–2212, doi:10.1002/2017GL076644, 2018.
- 7110 Cazenave, A.: Global sea-level budget 1993–present, *Earth Syst. Sci. Data*, 10, 1551–1590, doi:10.5194/essd-10-1551-2018, 2018.
- Cazenave, A., Dieng, H.-B., Meyssignac, B., Schuckmann, K. von, Decharme, B., and Berthier, E.: The rate of sea-level rise, *Nature Clim Change*, 4, 358–361, doi:10.1038/nclimate2159, 2014.
- Cazenave, A., Henry, O., Munier, S., Delcroix, T., Gordon, A. L., Meyssignac, B., Llovel, W., Palanisamy, H., and Becker, 7115 M.: Estimating ENSO Influence on the Global Mean Sea Level, 1993–2010, *Marine Geodesy*, 35, 82–97, doi:10.1080/01490419.2012.718209, 2012.
- Cazenave, A. and Llovel, W.: Contemporary sea level rise, *Annual review of marine science*, 2, 145–173, doi:10.1146/annurev-marine-120308-081105, 2010.
- Chambers, D. P., Cazenave, A., Champollion, N., Dieng, H., Llovel, W., Forsberg, R., Schuckmann, K. von, and Wada, Y.: 7120 Evaluation of the Global Mean Sea Level Budget between 1993 and 2014, *Surv Geophys*, 38, 309–327, doi:10.1007/s10712-016-9381-3, 2017.
- Chao, B. F., Wu, Y. H., and Li, Y. S.: Impact of artificial reservoir water impoundment on global sea level, *Science (New York, N.Y.)*, 320, 212–214, doi:10.1126/science.1154580, 2008.
- Cheng, M., Tapley, B. D., and Ries, J. C.: Deceleration in the Earth's oblateness, *J. Geophys. Res. Solid Earth*, 118, 740– 747, doi:10.1002/jgrb.50058, 2013.
- 7125 Church, J. A., Clark, P. U., Cazenave, A., Gregory, J. M., Jevrejeva, S., Levermann, A., Merrifield, M. A., Milne, G. A., Nerem, R. S., Nunn, P. D., Payne, A. J., Pfeffer, W. T., Stammer, D., and Unnikrishnan, A. S.: Sea level change. *Climate change 2013: the physical science basis. Contribution of working group I to the fifth assessment report of the intergovernmental panel on climate change*, Cambridge University Press, Cambridge, United Kingdom and New York, NY, USA, 1137–1216, 2013.
- 7130 Compo, G. P., Whitaker, J. S., Sardeshmukh, P. D., Matsui, N., Allan, R. J., Yin, X., Gleason, B. E., Vose, R. S., Rutledge, G., Bessemoulin, P., Brönnimann, S., Brunet, M., Crouthamel, R. I., Grant, A. N., Groisman, P. Y., Jones, P. D., Kruk, M. C., Kruger, A. C., Marshall, G. J., Maugeri, M., Mok, H. Y., Nordli, Ø., Ross, T. F., Trigo, R. M., Wang, X. L., Woodruff, S. D., and Worley, S. J.: The Twentieth Century Reanalysis Project, *Q.J.R. Meteorol. Soc.*, 137, 1–28, 7135 doi:10.1002/qj.776, 2011.
- Dee, D. P., Uppala, S. M., Simmons, A. J., Berrisford, P., Poli, P., Kobayashi, S., Andrae, U., Balmaseda, M. A., Balsamo, G., Bauer, P., Bechtold, P., Beljaars, A. C. M., van de Berg, L., Bidlot, J., Bormann, N., Delsol, C., Dragani, R., Fuentes, M., Geer, A. J., Haimberger, L., Healy, S. B., Hersbach, H., Hólm, E. V., Isaksen, I., Kållberg, P., Köhler, M., Matricardi, M., McNally, A. P., Monge-Sanz, B. M., Morcrette, J.-J., Park, B.-K., Peubey, C., Rosnay, P. de, Tavolato, 7140 C., Thépaut, J.-N., and Vitart, F.: The ERA-Interim reanalysis: configuration and performance of the data assimilation system, *Q.J.R. Meteorol. Soc.*, 137, 553–597, doi:10.1002/qj.828, 2011.



- Di Long, Pan, Y., Zhou, J., Chen, Y., Hou, X., Hong, Y., Scanlon, B. R., and Longuevergne, L.: Global analysis of spatiotemporal variability in merged total water storage changes using multiple GRACE products and global hydrological models, *Remote Sensing of Environment*, 192, 198–216, doi:10.1016/j.rse.2017.02.011, 2017.
- 7145 Dieng, H. B., Cazenave, A., Meyssignac, B., and Ablain, M.: New estimate of the current rate of sea level rise from a sea level budget approach, *Geophys. Res. Lett.*, 44, 3744–3751, doi:10.1002/2017GL073308, 2017.
- Dieng, H. B., Champollion, N., Cazenave, A., Wada, Y., Schrama, E., and Meyssignac, B.: Total land water storage change over 2003–2013 estimated from a global mass budget approach, *Environ. Res. Lett.*, 10, 124010, doi:10.1088/1748-9326/10/12/124010, 2015.
- 7150 Döll, P., Douville, H., Güntner, A., Müller Schmied, H., and Wada, Y.: Modelling Freshwater Resources at the Global Scale: Challenges and Prospects, *Surv Geophys*, 37, 195–221, doi:10.1007/s10712-015-9343-1, 2016.
- Döll, P., Fiedler, K., and Zhang, J.: Global-scale analysis of river flow alterations due to water withdrawals and reservoirs, *Hydrol. Earth Syst. Sci.*, 2009.
- Döll, P., Hoffmann-Dobrev, H., Portmann, F. T., Siebert, S., Eicker, A., Rodell, M., Strassberg, G., and Scanlon, B. R.: Impact of water withdrawals from groundwater and surface water on continental water storage variations, *Journal of Geodynamics*, 59-60, 143–156, doi:10.1016/j.jog.2011.05.001, 2012.
- 7155 Döll, P., Kaspar, F., and Lehner, B.: A global hydrological model for deriving water availability indicators: model tuning and validation, *Journal of Hydrology*, 2003.
- Döll, P. and Lehner, B.: Validation of a new global 30-min drainage direction map, *Journal of Hydrology*, 258, 214–231, doi:10.1016/S0022-1694(01)00565-0, 2002.
- 7160 Döll, P., Müller Schmied, H., Schuh, C., Portmann, F. T., and Eicker, A.: Global-scale assessment of groundwater depletion and related groundwater abstractions: Combining hydrological modeling with information from well observations and GRACE satellites, *Water Resour. Res.*, 50, 5698–5720, doi:10.1002/2014WR015595, 2014.
- Gelaro, R., McCarty, W., Suárez, M. J., Todling, R., Molod, A., Takacs, L., Randles, C. A., Darmenov, A., Bosilovich, M. G., Reichle, R., Wargan, K., Coy, L., Cullather, R., Draper, C., Akella, S., Buchard, V., Conaty, A., da Silva, A. M., Gu, W., Kim, G.-K., Koster, R., Lucchesi, R., Merkova, D., Nielsen, J. E., Partyka, G., Pawson, S., Putman, W., Rienecker, M., Schubert, S. D., Sienkiewicz, M., and Zhao, B.: The Modern-Era Retrospective Analysis for Research and Applications, Version 2 (MERRA-2), *J. Climate*, 30, 5419–5454, doi:10.1175/JCLI-D-16-0758.1, 2017.
- 7165 Gregory, J. M., White, N. J., Church, J. A., Bierkens, M. F. P., Box, J. E., van den Broeke, M. R., Cogley, J. G., Fettweis, X., Hanna, E., Huybrechts, P., Konikow, L. F., Leclercq, P. W., Marzeion, B., Oerlemans, J., Tamisiea, M. E., Wada, Y., Wake, L. M., and van de Wal, R. S. W.: Twentieth-Century Global-Mean Sea Level Rise: Is the Whole Greater than the Sum of the Parts?, *J. Climate*, 26, 4476–4499, doi:10.1175/JCLI-D-12-00319.1, 2013.
- 7170 Güntner, A.: Improvement of Global Hydrological Models Using GRACE Data, *Surv Geophys*, 29, 375–397, doi:10.1007/s10712-008-9038-y, 2008.

- 7175 Gutknecht, B. D., Groh, A., Cáceres, D., and Horwath, M.: Assessing Global Ocean and Continental Mass Change from 17 years of GRACE/-FO: the role of coastal buffer zones, 2020.
- Hanasaki, N., Kanae, S., and Oki, T.: A reservoir operation scheme for global river routing models, *Journal of Hydrology*, 327, 22–41, doi:10.1016/j.jhydrol.2005.11.011, 2006.
- Harris, I., Jones, P. D., Osborn, T. J., and Lister, D. H.: Updated high-resolution grids of monthly climatic observations - the CRU TS3.10 Dataset, *Int. J. Climatol.*, 34, 623–642, doi:10.1002/joc.3711, 2014.
- 7180 Hempel, S., Frieler, K., Warszawski, L., Schewe, J., and Piontek, F.: A trend-preserving bias correction &ndash; the ISI-MIP approach, *Earth Syst. Dynam.*, 4, 219–236, doi:10.5194/esd-4-219-2013, 2013.
- Hirabayashi, Y., Döll, P., and Kanae, S.: Global-scale modeling of glacier mass balances for water resources assessments: Glacier mass changes between 1948 and 2006, *Journal of Hydrology*, 390, 245–256, doi:10.1016/j.jhydrol.2010.07.001, 7185 2010.
- Hirabayashi, Y., Zang, Y., Watanabe, S., Koirala, S., and Kanae, S.: Projection of glacier mass changes under a high-emission climate scenario using the global glacier model HYOGA2, *Hydrological Research Letters*, 7, 6–11, doi:10.3178/hr.7.6, 2013.
- Hock, R., Bliss, A., Marzeion, B., GIESEN, R. H., Hirabayashi, Y., Huss, M., Radić, V., and SLANGEN, A. B. A.: 7190 GlacierMIP – A model intercomparison of global-scale glacier mass-balance models and projections, *J. Glaciol.*, 65, 453–467, doi:10.1017/jog.2019.22, 2019.
- Humphrey, V., Gudmundsson, L., and Seneviratne, S. I.: Assessing Global Water Storage Variability from GRACE: Trends, Seasonal Cycle, Subseasonal Anomalies and Extremes, *Surveys in geophysics*, 37, 357–395, doi:10.1007/s10712-016-9367-1, 2016.
- 7195 Huss, M. and Hock, R.: A new model for global glacier change and sea-level rise, *Front. Earth Sci.*, 3, 382, doi:10.3389/feart.2015.00054, 2015.
- Kauffeldt, A., Halldin, S., Rodhe, A., Xu, C.-Y., and Westerberg, I. K.: Disinformative data in large-scale hydrological modelling, *Hydrol. Earth Syst. Sci.*, 17, 2845–2857, doi:10.5194/hess-17-2845-2013, 2013.
- Kobayashi, S., OTA, Y., HARADA, Y., EBITA, A., MORIYA, M., ONODA, H., ONOGI, K., KAMAHORI, H., 7200 KOBAYASHI, C., ENDO, H., MIYAOKA, K., and TAKAHASHI, K.: The JRA-55 Reanalysis: General Specifications and Basic Characteristics, *Journal of the Meteorological Society of Japan*, 93, 5–48, doi:10.2151/jmsj.2015-001, 2015.
- Lawrence, D. M., Fisher, R. A., Koven, C. D., Oleson, K. W., Swenson, S. C., Bonan, G., Collier, N., Ghimire, B., Kampenhou, L., Kennedy, D., Kluzek, E., Lawrence, P. J., Li, F., Li, H., Lombardozzi, D., Riley, W. J., Sacks, W. J., Shi, M., Vertenstein, M., Wieder, W. R., Xu, C., Ali, A. A., Badger, A. M., Bisht, G., Broeke, M., Brunke, M. A., Burns, 7205 S. P., Buzan, J., Clark, M., Craig, A., Dahlin, K., Drewniak, B., Fisher, J. B., Flanner, M., Fox, A. M., Gentine, P., Hoffman, F., Keppel-Aleks, G., Knox, R., Kumar, S., Lenaerts, J., Leung, L. R., Lipscomb, W. H., Lu, Y., Pandey, A., Pelletier, J. D., Perket, J., Randerson, J. T., Ricciuto, D. M., Sanderson, B. M., Slater, A., Subin, Z. M., Tang, J.,

- Thomas, R. Q., Val Martin, M., and Zeng, X.: The Community Land Model version 5: Description of new features, benchmarking, and impact of forcing uncertainty, *J. Adv. Model. Earth Syst.*, doi:10.1029/2018MS001583, 2019.
- 7210 Lehner, B., Liermann, C. R., Revenga, C., Vörösmarty, C., Fekete, B., Crouzet, P., Döll, P., Endejan, M., Frenken, K., Magome, J., Nilsson, C., Robertson, J. C., Rödel, R., Sindorf, N., and Wisser, D.: High-resolution mapping of the world's reservoirs and dams for sustainable river-flow management, *Frontiers in Ecology and the Environment*, 9, 494–502, doi:10.1890/100125, 2011.
- Llovel, W., Becker, M., Cazenave, A., Jevrejeva, S., Alkama, R., Decharme, B., Douville, H., Ablain, M., and Beckley, B.: Terrestrial waters and sea level variations on interannual time scale, *Global and Planetary Change*, 75, 76–82, doi:10.1016/j.gloplacha.2010.10.008, 2011.
- 7215 Marzeion, B., Jarosch, A. H., and Hofer, M.: Past and future sea-level change from the surface mass balance of glaciers, *The Cryosphere*, 6, 1295–1322, doi:10.5194/tc-6-1295-2012, 2012.
- Marzeion, B., Leclercq, P. W., Cogley, J. G., and Jarosch, A. H.: Brief Communication: Global reconstructions of glacier mass change during the 20th century are consistent, *The Cryosphere*, 9, 2399–2404, doi:10.5194/tc-9-2399-2015, 2015.
- 7220 Mayer-Gürr, T., Behzadpur, S., Ellmer, M., Kvas, A., Klinger, B., Strasser, S., and Zehentner, N.: ITSG-Grace2018 - Monthly, Daily and Static Gravity Field Solutions from GRACE, 2018.
- Milly, P. C. D. C., Cazenave, A., Famiglietti, J. S., Gornitz, V., Laval, K., Lettenmaier, D. P., Sahagian, D. L., Wahr, J. M., and Wilson, C. R.: Terrestrial Water-Storage Contributions to Sea-Level Rise and Variability, in: *Understanding Sea-level rise and variability*, Church, J. A. (Ed.), John Wiley & Sons, Chichester, 226–255, 2010.
- 7225 Müller Schmied, H., Adam, L., Eisner, S., Fink, G., Flörke, M., Kim, H., Oki, T., Portmann, F. T., Reinecke, R., Riedel, C., Song, Q., Zhang, J., and Döll, P.: Variations of global and continental water balance components as impacted by climate forcing uncertainty and human water use, *Hydrol. Earth Syst. Sci.*, 20, 2877–2898, doi:10.5194/hess-20-2877-2016, 2016.
- 7230 Müller Schmied, H., Eisner, S., Franz, D., Wattenbach, M., Portmann, F. T., Flörke, M., and Döll, P.: Sensitivity of simulated global-scale freshwater fluxes and storages to input data, hydrological model structure, human water use and calibration, *Hydrol. Earth Syst. Sci.*, 18, 3511–3538, doi:10.5194/hess-18-3511-2014, 2014.
- Munier, S., Palanisamy, H., Maisongrande, P., Cazenave, A., and Wood, E. F.: Global runoff anomalies over 1993–2009 estimated from coupled Land–Ocean–Atmosphere water budgets and its relation with climate variability, *Hydrol. Earth Syst. Sci.*, 16, 3647–3658, doi:10.5194/hess-16-3647-2012, 2012.
- 7235 Nash, J. E. and Sutcliffe, J. V.: River flow forecasting through conceptual models part I — A discussion of principles, *Journal of Hydrology*, 10, 282–290, doi:10.1016/0022-1694(70)90255-6, 1970.
- New, M., Hulme, M., and Jones, P.: Representing Twentieth-Century Space–Time Climate Variability. Part II: Development of 1901–96 Monthly Grids of Terrestrial Surface Climate, *J. Climate*, 13, 2217–2238, doi:10.1175/1520-0442(2000)013<2217:RTCSTC>2.0.CO;2, 2000.
- 7240

- New, M., Lister, D., Hulme, M., and Makin, I.: A high-resolution data set of surface climate over global land areas, *Clim. Res.*, 21, 1–25, doi:10.3354/cr021001, 2002.
- 7245 Oppenheimer, M., Hinkel, J., van de Wal, R., Magnan, A. K., Abd-Elgawad, A., Cai, R., Cifuentes-Jara, M., Deconto, R. M., Ghosh, T., Hay, J., Isla, F., Marzeion, B., Meyssignac, B., Sebesvari, Z., and Glavovic, B.: Sea Level Rise and Implications for Low Lying Islands, Coasts and Communities, Chapter 4 of the IPCC Special Report on the Ocean and Cryosphere in a Changing Climate, 169 pp., 2019.
- Pfeffer, W. T., Arendt, A. A., Bliss, A., Bolch, T., Cogley, J. G., Gardner, A. S., Hagen, J.-O., Hock, R., Kaser, G., Kienholz, C., Miles, E. S., Moholdt, G., Mölg, N., Paul, F., Radić, V., Rastner, P., Raup, B. H., Rich, J., and Sharp, M. J.: The Randolph Glacier Inventory: a globally complete inventory of glaciers, *J. Glaciol.*, 60, 537–552, doi:10.3189/2014JoG13J176, 2014.
- 7250 Poli, P., Hersbach, H., Dee, D. P., Berrisford, P., Simmons, A. J., Vitart, F., Laloyaux, P., Tan, D. G. H., Peubey, C., Thépaut, J.-N., Trémolet, Y., Hólm, E. V., Bonavita, M., Isaksen, L., and Fisher, M.: ERA-20C: An Atmospheric Reanalysis of the Twentieth Century, *J. Climate*, 29, 4083–4097, doi:10.1175/JCLI-D-15-0556.1, 2016.
- 7255 Reager, J. T., Gardner, A. S., Famiglietti, J. S., Wiese, D. N., Eicker, A., and Lo, M.-H.: A decade of sea level rise slowed by climate-driven hydrology, *Science (New York, N.Y.)*, 351, 699–703, doi:10.1126/science.aad8386, 2016.
- Rietbroek, R., Brunnabend, S.-E., Kusche, J., Schröter, J., and Dahle, C.: Revisiting the contemporary sea-level budget on global and regional scales, *Proceedings of the National Academy of Sciences of the United States of America*, 113, 1504–1509, doi:10.1073/pnas.1519132113, 2016.
- Rost, S., Gerten, D., Bondeau, A., Lucht, W., Rohwer, J., and Schaphoff, S.: Agricultural green and blue water consumption and its influence on the global water system, *Water Resour. Res.*, 44, doi:10.1029/2007WR006331, 2008.
- 7260 Saha, S., Moorthi, S., Pan, H.-L., Wu, X., Wang, J., Nadiga, S., Tripp, P., Kistler, R., Woollen, J., Behringer, D., Liu, H., Stokes, D., Grumbine, R., Gayno, G., Wang, J., Hou, Y.-T., Chuang, H.-y., Juang, H.-M. H., Sela, J., Iredell, M., Treadon, R., Kleist, D., van Delst, P., Keyser, D., Derber, J., Ek, M., Meng, J., Wei, H., Yang, R., Lord, S., van den Dool, H., Kumar, A., Wang, W., Long, C., Chelliah, M., Xue, Y., Huang, B., Schemm, J.-K., Ebisuzaki, W., Lin, R., Xie, P., Chen, M., Zhou, S., Higgins, W., Zou, C.-Z., Liu, Q., Chen, Y., Han, Y., Cucurull, L., Reynolds, R. W., Rutledge, G., and Goldberg, M.: The NCEP Climate Forecast System Reanalysis, *Bull. Amer. Meteor. Soc.*, 91, 1015–1058, doi:10.1175/2010BAMS3001.1, 2010.
- 7265 Saha, S., Moorthi, S., Wu, X., Wang, J., Nadiga, S., Tripp, P., Behringer, D., Hou, Y.-T., Chuang, H.-y., Iredell, M., Ek, M., Meng, J., Yang, R., Mendez, M. P., van den Dool, H., Zhang, Q., Wang, W., Chen, M., and Becker, E.: The NCEP Climate Forecast System Version 2, *J. Climate*, 27, 2185–2208, doi:10.1175/JCLI-D-12-00823.1, 2014.
- 7270 Scanlon, B. R., Zhang, Z., Rateb, A., Sun, A., Wiese, D., Save, H., Beaudoin, H., Lo, M. H., Müller-Schmied, H., Döll, P., Beek, R., Swenson, S., Lawrence, D., Croteau, M., and Reedy, R. C.: Tracking Seasonal Fluctuations in Land Water Storage Using Global Models and GRACE Satellites, *Geophys. Res. Lett.*, 6, 3, doi:10.1029/2018GL081836, 2019.

- Scanlon, B. R., Zhang, Z., Save, H., Sun, A. Y., Müller Schmied, H., van Beek, L. P. H., Wiese, D. N., Wada, Y., Di Long,  
7275 Reedy, R. C., Longuevergne, L., Döll, P., and Bierkens, M. F. P.: Global models underestimate large decadal declining  
and rising water storage trends relative to GRACE satellite data, *Proceedings of the National Academy of Sciences of  
the United States of America*, 115, E1080-E1089, doi:10.1073/pnas.1704665115, 2018.
- Schneider, U., Becker, A., Finger, P., Meyer-Christoffer, A., Rudolf, B., and Ziese, M.: GPCP Full Data Reanalysis Version  
7.0 at 0.5°: Monthly Land-Surface Precipitation from Rain-Gauges built on GTS-based and Historic Data, Research  
7280 Data Archive at the National Center for Atmospheric Research, Computational and Information Systems Laboratory,  
Boulder, Colo. (Updated irregularly.), doi:10.5676/DWD\_GPCP/FD\_M\_V7\_050, 2015.
- Schneider, U., Becker, A., Finger, P., Meyer-Christoffer, A., Ziese, M., and Rudolf, B.: GPCP's new land surface  
precipitation climatology based on quality-controlled in situ data and its role in quantifying the global water cycle, *Theor  
Appl Climatol*, 115, 15–40, doi:10.1007/s00704-013-0860-x, 2014.
- 7285 Schrama, E. J. O., Wouters, B., and Rietbroek, R.: A mascon approach to assess ice sheet and glacier mass balances and their  
uncertainties from GRACE data, *J. Geophys. Res. Solid Earth*, 119, 6048–6066, doi:10.1002/2013JB010923, 2014.
- Siebert, S., Burke, J., Faures, J. M., Frenken, K., Hoogeveen, J., Döll, P., and Portmann, F. T.: Groundwater use for  
irrigation – a global inventory, *Hydrol. Earth Syst. Sci.*, 14, 1863–1880, doi:10.5194/hess-14-1863-2010, 2010.
- Slangen, A. B. A., Adloff, F., Jevrejeva, S., Leclercq, P. W., Marzeion, B., Wada, Y., and Winkelmann, R.: A Review of  
7290 Recent Updates of Sea-Level Projections at Global and Regional Scales, *Surv Geophys*, 38, 385–406,  
doi:10.1007/s10712-016-9374-2, 2017.
- Slangen, A. B. A., Church, J. A., Agosta, C., Fettweis, X., Marzeion, B., and Richter, K.: Anthropogenic forcing dominates  
global mean sea-level rise since 1970, *Nature Clim Change*, 6, 701–705, doi:10.1038/nclimate2991, 2016.
- Sutanudjaja, E. H., van Beek, R., Wanders, N., Wada, Y., Bosmans, J. H. C., Drost, N., van der Ent, R. J., Graaf, I. E. M. de,  
7295 Hoch, J. M., Jong, K. de, Karssenberg, D., López López, P., Peßenteiner, S., Schmitz, O., Straatsma, M. W.,  
Vannamettee, E., Wisser, D., and Bierkens, M. F. P.: PCR-GLOBWB 2: a 5 arcmin global hydrological and water  
resources model, *Geosci. Model Dev.*, 11, 2429–2453, doi:10.5194/gmd-11-2429-2018, 2018.
- Swenson, S., Chambers, D., and Wahr, J.: Estimating geocenter variations from a combination of GRACE and ocean model  
output, *J. Geophys. Res. Solid Earth*, 113, 29,077, doi:10.1029/2007JB005338, 2008.
- 7300 Tangdamrongsub, N., Han, S.-C., Tian, S., Müller Schmied, H., Sutanudjaja, E. H., Ran, J., and Feng, W.: Evaluation of  
Groundwater Storage Variations Estimated from GRACE Data Assimilation and State-of-the-Art Land Surface Models  
in Australia and the North China Plain, *Remote Sensing*, 10, 483, doi:10.3390/rs10030483, 2018.
- van Dijk, A. I. J. M., Renzullo, L. J., Wada, Y., and Tregoning, P.: A global water cycle reanalysis (2003–2012) merging  
satellite gravimetry and altimetry observations with a hydrological multi-model ensemble, *Hydrol. Earth Syst. Sci.*, 18,  
7305 2955–2973, doi:10.5194/hess-18-2955-2014, 2014.
- Wada, Y., Lo, M.-H., Yeh, P. J.-F., Reager, J. T., Famiglietti, J. S., Wu, R.-J., and Tseng, Y.-H.: Fate of water pumped from  
underground and contributions to sea-level rise, *Nature Clim Change*, 6, 777–780, doi:10.1038/nclimate3001, 2016.

- 7310 Wada, Y., Reager, J. T., Chao, B. F., Wang, J., Lo, M.-H., Song, C., Li, Y., and Gardner, A. S.: Recent Changes in Land Water Storage and its Contribution to Sea Level Variations, *Surv Geophys*, 38, 131–152, doi:10.1007/s10712-016-9399-6, 2017.
- Wang, J., Song, C., Reager, J. T., Yao, F., Famiglietti, J. S., Sheng, Y., MacDonald, G. M., Brun, F., Schmied, H. M., Marston, R. A., and Wada, Y.: Recent global decline in endorheic basin water storages, *Nature geoscience*, 11, 926–932, doi:10.1038/s41561-018-0265-7, 2018.
- 7315 Weedon, G. P., Balsamo, G., Bellouin, N., Gomes, S., Best, M. J., and Viterbo, P.: The WFDEI meteorological forcing data set: WATCH Forcing Data methodology applied to ERA-Interim reanalysis data, *Water Resour. Res.*, 50, 7505–7514, doi:10.1002/2014WR015638, 2014.
- Weedon, G. P., Gomes, S., Viterbo, P., Shuttleworth, W. J., Blyth, E., Österle, H., Adam, J. C., Bellouin, N., Boucher, O., and Best, M.: Creation of the WATCH Forcing Data and Its Use to Assess Global and Regional Reference Crop Evaporation over Land during the Twentieth Century, *J. Hydrometeor*, 12, 823–848, doi:10.1175/2011JHM1369.1, 2011.
- 7320 Werth, S. and Güntner, A.: Calibration analysis for water storage variability of the global hydrological model WGHM, *Hydrol. Earth Syst. Sci.*, 14, 59–78, doi:10.5194/hess-14-59-2010, 2010.
- Wolter, K. and Timlin, M. S.: Monitoring ENSO in COADS with a seasonally adjusted principal component index, *Proceedings of the 17th Climate Diagnostics Workshop*, 52–57, 1993.
- 7325 Wolter, K. and Timlin, M. S.: Measuring the strength of ENSO events: How does 1997/98 rank?, *Weather*, 53, 315–324, doi:10.1002/j.1477-8696.1998.tb06408.x, 1998.
- World Glacier Monitoring Service: Fluctuations of Glaciers Database, 2016.
- World Glacier Monitoring Service: Fluctuations of Glaciers Database, 2017.
- 7330 Zemp, M., Huss, M., Thibert, E., Eckert, N., McNabb, R., Huber, J., Barandun, M., Machguth, H., Nussbaumer, S. U., Gärtner-Roer, I., Thomson, L., Paul, F., Maussion, F., Kutuzov, S., and Cogley, J. G.: Global glacier mass changes and their contributions to sea-level rise from 1961 to 2016, *Nature*, 568, 382–386, doi:10.1038/s41586-019-1071-0, 2019.



Page 4: [2] Deleted	Denise Caceres	01/05/2020 15:22:00
Page 4: [2] Deleted	Denise Caceres	01/05/2020 15:22:00
Page 4: [2] Deleted	Denise Caceres	01/05/2020 15:22:00
Page 4: [2] Deleted	Denise Caceres	01/05/2020 15:22:00
Page 4: [2] Deleted	Denise Caceres	01/05/2020 15:22:00
Page 4: [2] Deleted	Denise Caceres	01/05/2020 15:22:00
Page 4: [2] Deleted	Denise Caceres	01/05/2020 15:22:00
Page 4: [2] Deleted	Denise Caceres	01/05/2020 15:22:00
Page 4: [2] Deleted	Denise Caceres	01/05/2020 15:22:00
Page 4: [2] Deleted	Denise Caceres	01/05/2020 15:22:00
Page 4: [2] Deleted	Denise Caceres	01/05/2020 15:22:00
Page 4: [2] Deleted	Denise Caceres	01/05/2020 15:22:00
Page 4: [2] Deleted	Denise Caceres	01/05/2020 15:22:00
Page 4: [2] Deleted	Denise Caceres	01/05/2020 15:22:00
Page 4: [2] Deleted	Denise Caceres	01/05/2020 15:22:00
Page 4: [2] Deleted	Denise Caceres	01/05/2020 15:22:00
Page 4: [2] Deleted	Denise Caceres	01/05/2020 15:22:00
Page 4: [2] Deleted	Denise Caceres	01/05/2020 15:22:00
Page 4: [2] Deleted	Denise Caceres	01/05/2020 15:22:00
Page 4: [2] Deleted	Denise Caceres	01/05/2020 15:22:00
Page 4: [2] Deleted	Denise Caceres	01/05/2020 15:22:00
Page 4: [3] Deleted	Institut für physische Geographie	04/05/2020 15:30:00

Page 4: [3] Deleted	Institut für physische Geographie	04/05/2020 15:30:00
---------------------	-----------------------------------	---------------------

Page 4: [3] Deleted	Institut für physische Geographie	04/05/2020 15:30:00
---------------------	-----------------------------------	---------------------

Page 9: [4] Deleted	Denise Caceres	27/06/2020 15:12:00
Page 10: [5] Deleted	Denise Caceres	14/04/2020 10:28:00
Page 10: [5] Deleted	Denise Caceres	14/04/2020 10:28:00
Page 10: [5] Deleted	Denise Caceres	14/04/2020 10:28:00
Page 10: [5] Deleted	Denise Caceres	14/04/2020 10:28:00
Page 10: [5] Deleted	Denise Caceres	14/04/2020 10:28:00







Page 10: [14] Deleted	Denise Caceres	14/04/2020 10:33:00
Page 10: [14] Deleted	Denise Caceres	14/04/2020 10:33:00
Page 10: [14] Deleted	Denise Caceres	14/04/2020 10:33:00
Page 10: [14] Deleted	Denise Caceres	14/04/2020 10:33:00
Page 10: [14] Deleted	Denise Caceres	14/04/2020 10:33:00
Page 10: [14] Deleted	Denise Caceres	14/04/2020 10:33:00
Page 10: [14] Deleted	Denise Caceres	14/04/2020 10:33:00
Page 10: [14] Deleted	Denise Caceres	14/04/2020 10:33:00
Page 10: [14] Deleted	Denise Caceres	14/04/2020 10:33:00
Page 10: [14] Deleted	Denise Caceres	14/04/2020 10:33:00
Page 10: [14] Deleted	Denise Caceres	14/04/2020 10:33:00
Page 10: [14] Deleted	Denise Caceres	14/04/2020 10:33:00
Page 10: [14] Deleted	Denise Caceres	14/04/2020 10:33:00
Page 10: [14] Deleted	Denise Caceres	14/04/2020 10:33:00
Page 10: [14] Deleted	Denise Caceres	14/04/2020 10:33:00
Page 10: [14] Deleted	Denise Caceres	14/04/2020 10:33:00
Page 10: [14] Deleted	Denise Caceres	14/04/2020 10:33:00
Page 10: [14] Deleted	Denise Caceres	14/04/2020 10:33:00
Page 10: [14] Deleted	Denise Caceres	14/04/2020 10:33:00
Page 10: [14] Deleted	Denise Caceres	14/04/2020 10:33:00
Page 14: [15] Deleted	Denise Caceres	06/04/2020 12:12:00

▼

Page 14: [16] Deleted	Denise Caceres	06/04/2020 12:18:00
Page 17: [17] Deleted	Denise Caceres	06/05/2020 17:00:00

▼

Page 17: [18] Deleted	Denise Caceres	06/05/2020 16:59:00
Page 18: [19] Deleted	Denise Caceres	29/05/2020 11:52:00

▼

Page 19: [20] Deleted	Denise Caceres	29/05/2020 11:56:00
-----------------------	----------------	---------------------

▼

**Page 19: [23] Deleted** **Denise Caceres** **29/05/2020 11:56:00**



**Page 19: [24] Deleted** **Denise Caceres** **29/05/2020 12:27:00**



**Page 19: [25] Deleted** **Denise Caceres** **29/05/2020 12:26:00**



**Page 19: [26] Deleted** **Denise Caceres** **29/05/2020 12:26:00**



**Page 19: [27] Deleted** **Denise Caceres** **29/05/2020 12:26:00**



**Page 19: [28] Deleted** **Denise Caceres** **29/05/2020 12:26:00**



**Page 27: [29] Deleted** **Denise Caceres** **29/05/2020 11:53:00**



**Page 27: [29] Deleted** **Denise Caceres** **29/05/2020 11:53:00**



**Page 27: [30] Deleted** **Denise Caceres** **24/06/2020 11:47:00**



**Page 27: [30] Deleted** **Denise Caceres** **24/06/2020 11:47:00**



**Page 27: [30] Deleted** **Denise Caceres** **24/06/2020 11:47:00**



**Page 27: [30] Deleted** **Denise Caceres** **24/06/2020 11:47:00**



**Page 27: [32] Deleted Denise Caceres 29/06/2020 12:19:00**



**Page 27: [32] Deleted Denise Caceres 29/06/2020 12:19:00**



**Page 27: [32] Deleted Denise Caceres 29/06/2020 12:19:00**



**Page 27: [32] Deleted Denise Caceres 29/06/2020 12:19:00**



**Page 27: [33] Deleted Denise Caceres 06/04/2020 12:29:00**



**Page 27: [33] Deleted Denise Caceres 06/04/2020 12:29:00**



**Page 27: [33] Deleted Denise Caceres 06/04/2020 12:29:00**



**Page 27: [33] Deleted Denise Caceres 06/04/2020 12:29:00**



**Page 27: [34] Deleted Denise Caceres 29/06/2020 13:52:00**



**Page 27: [34] Deleted Denise Caceres 29/06/2020 13:52:00**



**Page 27: [34] Deleted Denise Caceres 29/06/2020 13:52:00**



**Page 27: [34] Deleted Denise Caceres 29/06/2020 13:52:00**



**Page 27: [34] Deleted Denise Caceres 29/06/2020 13:52:00**

